Surface receptor Toso controls B cell–mediated regulation of T cell immunity

Jinbo Yu, Vu Huy Hoang Duong, Katrin Westphal, Andreas Westphal, Abdulhadi Suwandi, Guntram A. Grassl, Korbinian Brand, Andrew C. Chan, Niko Föger, Kyeong-Hee Lee

Research Article   Immunology   Inflammation

The immune system is tightly controlled by regulatory processes that allow for the elimination of invading pathogens, while limiting immunopathological damage to the host. In the present study, we found that conditional deletion of the cell surface receptor Toso on B cells unexpectedly resulted in impaired proinflammatory T cell responses, which led to impaired immune protection in an acute viral infection model and was associated with reduced immunopathological tissue damage in a chronic inflammatory context. Toso exhibited its B cell–inherent immunoregulatory function by negatively controlling the pool of IL-10–competent B1 and B2 B cells, which were characterized by a high degree of self-reactivity and were shown to mediate immunosuppressive activity on inflammatory T cell responses in vivo. Our results indicate that Toso is involved in the differentiation/maintenance of regulatory B cells by fine-tuning B cell receptor activation thresholds. Furthermore, we showed that during influenza A–induced pulmonary inflammation, the application of Toso-specific antibodies selectively induced IL-10–competent B cells at the site of inflammation and resulted in decreased proinflammatory cytokine production by lung T cells. These findings suggest that Toso may serve as a novel therapeutic target to dampen pathogenic T cell responses via the modulation of IL-10–competent regulatory B cells.

Find the latest version:

https://jci.me/97280/pdf

Surface receptor Toso controls B cell–mediated regulation of T cell immunity

Jinbo Yu,[1,2] Vu Huy Hoang Duong,[1,2] Katrin Westphal,[1,2] Andreas Westphal,[1,2] Abdulhadi Suwandi,[3] Guntram A. Grassl,[3] Korbinian Brand,[2] Andrew C. Chan,[4] Niko Föger,[1,2] and Kyeong-Hee Lee[1,2]

[1]Inflammation Research Group, [2]Institute of Clinical Chemistry, and [3]Institute of Medical Microbiology and Hospital Epidemiology and German Center for Infection Research (DZIF), Hannover Medical School, Hannover, Germany. [4]Research, Genentech, South San Francisco, California, USA.

The immune system is tightly controlled by regulatory processes that allow for the elimination of invading pathogens, while limiting immunopathological damage to the host. In the present study, we found that conditional deletion of the cell surface receptor Toso on B cells unexpectedly resulted in impaired proinflammatory T cell responses, which led to impaired immune protection in an acute viral infection model and was associated with reduced immunopathological tissue damage in a chronic inflammatory context. Toso exhibited its B cell–inherent immunoregulatory function by negatively controlling the pool of IL-10–competent B1 and B2 B cells, which were characterized by a high degree of self-reactivity and were shown to mediate immunosuppressive activity on inflammatory T cell responses in vivo. Our results indicate that Toso is involved in the differentiation/maintenance of regulatory B cells by fine-tuning B cell receptor activation thresholds. Furthermore, we showed that during influenza A–induced pulmonary inflammation, the application of Toso-specific antibodies selectively induced IL-10–competent B cells at the site of inflammation and resulted in decreased proinflammatory cytokine production by lung T cells. These findings suggest that Toso may serve as a novel therapeutic target to dampen pathogenic T cell responses via the modulation of IL-10–competent regulatory B cells.

Introduction

A key feature of the immune system is the maintenance of a delicate balance between protecting against infectious agents and minimizing immune-mediated tissue damage. To achieve this critical equilibrium, tight regulatory mechanisms have evolved to control protective immune responses and to avoid misguided or excessive inflammation. It is now well established that a subset of CD4^{+} T cells, termed regulatory T cells, exhibit immunosuppressive function and are crucial for the maintenance of normal immune homeostasis by controlling inflammation and preventing autoimmunity (1). More recently, it has been recognized that B cells can also negatively regulate T cell responses in an antibody-independent manner. A suppressive role of B cells in pathogenic T cell responses was already suggested in 1996 by Janeway and colleagues, who showed that B cell–deficient mice exhibited exacerbated disease in experimental autoimmune encephalomyelitis (EAE) (2). An increasing number of reports has since indicated immunoregulatory function of B cells in various disease models, including T cell–dependent autoimmune models (3–8), transplantation (9), inflammation (10), and cancer (11), which has led to the concept of regulatory B cells (Bregs). Bregs exhibit their regulatory function primarily via the release of IL-10, although other mechanisms may also be involved (12). In vivo identification

of Bregs is complicated by the description of multiple different Breg subsets with partially overlapping phenotypes and surface marker characteristics in different mouse and human model systems (13). Until now, no Breg-defining transcription factor or unique lineage marker has been identified, and Bregs are mainly defined by their ability to secrete IL-10. The nature and origin of Bregs are still controversial, and it is unclear whether they represent a distinct B cell lineage or a dynamic cellular state.

Toso, also known as Faim3 (Fas apoptosis inhibitory molecule 3) or FcμR (Fc receptor for IgM), is a type I transmembrane protein belonging to the immunoglobulin gene superfamily. Expression of Toso is restricted to lymphoid organs, where it is particularly highly expressed in B cells. In humans, a tight association of Toso overexpression with B cell malignancy has been observed in patients with chronic lymphocytic leukemia (14–16). Toso was originally identified as a surface molecule with negative regulatory function on lymphocyte apoptosis (17, 18). Subsequently, additional studies have identified Toso as an Fc receptor for soluble IgM (Fcμ receptor) (19, 20). More recently, it has been demonstrated that Toso physically interacts with membrane IgM-containing B cell antigen receptor (BCR) complexes on the surface of mature B cells and/or within the *trans*-Golgi network of developing B cells (21, 22). Functionally, increasing evidence suggests that Toso serves as a physiologically important immunoregulatory molecule for B and T cells. Toso-deficient mice have been reported to show enhanced serum levels of IgM and IgG autoantibodies (21, 23–25), which, however, are not associated with autoimmune pathology (26). Furthermore, studies on Toso-deficient mice have revealed strong immunoprotective function of Toso in a model of *Listeria* infection (27) and during lymphocytic choriomeningitis

virus infection (28). Toso-deficient mice are also largely resistant to the development of EAE and exhibit reduced pathogenic T cell responses (29). The mechanism underlying the phenotypic defects of Toso-deficient mice remains a controversial issue, and models involving different effector mechanisms and different immune cell types have been proposed (21, 22, 27, 29). Particularly, it is unclear whether the effects of Toso on tolerance in the B cell compartment are interrelated with impaired immune protection in Toso-deficient mice.

We demonstrate here that the specific deletion of Toso on B cells results in impaired antiviral T cell responses. We provide evidence that links this immunoregulatory function of B cells on T cell immunity to a specific set of IL-10–competent B cells. Our data show that these Bregs are negatively regulated by Toso and exhibit high prevalence for self-reactivity. Thus, via control of the pool of Bregs, Toso exhibits a dual role in immune homeostasis: it maintains normal self-tolerance within the B cell compartment and, at the same time, ensures protective T cell immunity against infection.

Results

Toso deficiency results in increased mortality and reduced production of proinflammatory cytokines by T cells upon influenza infection. To assess the impact of Toso on immune responses during acute viral infection, we intranasally infected WT and Toso$^{-/-}$ mice with 1,000 PFU of influenza virus strain A/PR8 (H1N1). Whereas 84% of WT animals survived infection, Toso$^{-/-}$ mice exhibited significantly increased mortality; most died between days 10 and 15 postinfection (p.i.), and only 23% survived (Figure 1A). Pulmonary viral titers in the bronchoalveolar lavage fluid were comparable between WT and Toso$^{-/-}$ mice at day 4 p.i., indicating normal viral replication and infectivity, but were relatively increased in Toso$^{-/-}$ mice during the clearance phase (day 7 p.i.) (Supplemental Figure 1A; supplemental material available online with this article; https://doi.org/10.1172/JCI97280DS1). Thus, increased influenza-induced mortality of Toso$^{-/-}$ mice was associated with delayed viral clearance.

Antiviral immunity and recovery from influenza infection are largely dependent on effector T cell responses (30, 31), which usually peak around days 9–10 p.i., just when Toso$^{-/-}$ mice start to become moribund. We thus next examined virus-specific T cell responses in Toso$^{-/-}$ mice. Viral antigen-specific CD4$^+$ and CD8$^+$ T cell populations were enumerated in the lungs of infected animals at day 9 p.i. by tetramer staining for the immunodominant CD4 T cell epitope NP$_{311–325}$/I-A^b (NP311) or the CD8 T cell epitope NP$_{366–374}$/D^b (NP366). Both frequency and absolute numbers of virus-specific NP311-tetramer–positive CD4$^+$ T cells and NP366-dextramer–positive CD8$^+$ T cells were comparable between WT and Toso$^{-/-}$ mice (Figure 1, B and C), indicating normal antigen-specific priming and clonal expansion of virus-specific T cells in Toso$^{-/-}$ mice.

Effector T cells contribute to viral control and elimination by the production of potent proinflammatory cytokines such as TNF-α and IFN-γ. The percentage as well as absolute numbers of IFN-γ– and TNF-α–producing T cells from lungs of influenza A–infected mice was significantly reduced in Toso$^{-/-}$ mice with both CD4$^+$ and CD8$^+$ T cells being affected (Figure 1, D–G).

Reduced production of these important antiviral cytokines (IFN-γ and TNF-α) by Toso$^{-/-}$ T cells was also observed in the spleen of infected animals, irrespective of whether mice were infected with a high dose (1,000 PFU) or a low dose (50 PFU) of influenza virus (Supplemental Figure 1, B–G, and data not shown), the latter not inducing any mortality in WT or Toso$^{-/-}$ mice.

Thus, although T cells in Toso$^{-/-}$ mice were capable of being activated and expanding in response to viral infection, these T cells were compromised in mounting an efficient antiviral cytokine response.

Conditional deletion of Toso in B cells results in impaired protective T cell immunity and limits immunopathological tissue damage. To assess whether reduced production of proinflammatory cytokines by T cells in Toso$^{-/-}$ mice is a T cell–intrinsic defect that depends on the specific deletion of Toso in T cells, or whether this is an indirect effect mediated by other cell types, such as antigen-presenting dendritic cells or B cells, we used a conditional gene targeting approach. To this end, we crossed Toso$^{f/f}$ mice onto different Cre-recombinase–expressing transgenic mouse lines — CD4-Cre mice, CD11c-Cre mice, and CD19-Cre mice — to specifically delete Toso in T cells, dendritic cells, and B cells, respectively (Supplemental Figure 2).

Upon influenza A infection, virus-induced mortality, as well as IFN-γ and TNF-α production by T cells, was not affected by ablation of Toso in T cells (Toso$^{f/f}$/CD4-Cre$^{+/-}$ mice) (Figure 2A and Supplemental Figure 3, A–D). Overall survival and T cell responses were also normal in Toso$^{f/f}$/CD11c-Cre$^{+/-}$ mice (Figure 2B and Supplemental Figure 3, E–H), indicating that conditional deletion of Toso in dendritic cells does not compromise their capacity to efficiently prime T cell activation. To our surprise, increased virus-induced lethality and impaired production of proinflammatory cytokines by T cells were only observed upon specific deletion of Toso in B cells (Toso$^{f/f}$/CD19-Cre$^{+/-}$ mice) (Figure 2, C–G). Similarly to straight Toso$^{-/-}$ mice (Figure 1A), most Toso$^{f/f}$/CD19-Cre$^{+/-}$ mice died between days 10 and 15 p.i. (only 11% survival), whereas 88% of CD19-Cre$^{+/-}$ control mice survived infection (Figure 2C). Also, the functional ability of CD4$^+$ and CD8$^+$ T cells to produce IFN-γ and TNF-α was significantly impaired in Toso$^{f/f}$/CD19-Cre$^{+/-}$ mice compared with CD19-Cre$^{+/-}$ control mice (Figure 2, D–G). These data strongly indicate that the functional defect of T cells in Toso-deficient mice is not a T cell–intrinsic phenotype, but rather is indirectly induced by Toso-deficient B cells. Upon influenza infection, Toso$^{f/f}$/CD19-Cre$^{+/-}$ mice also had significantly more CD4$^+$ T cells expressing PD-1 (Figure 2H and Supplemental Figure 4A), an inhibitory surface receptor that has been associated with T cell exhaustion (32). Interestingly, increased PD-1 expression on CD4$^+$ T cells upon Toso deletion in B cells correlated with increased expression of its cognate ligand PD-L2 on CD19$^+$ B cells (Figure 2I and Supplemental Figure 4B).

We further extended our studies on the B cell–specific role of Toso to a model of infection-induced intestinal pathology, using infection with attenuated *Salmonella* Typhimurium. In this model, chronic *Salmonella* infection of the murine gastrointestinal tract is associated with severe immunopathology that manifests in tissue fibrosis and extensive damage to the gut tissue along with the expression of a characteristic Th1-dominated inflammatory cytokine profile (33). Using this model, conditional deletion of Toso on
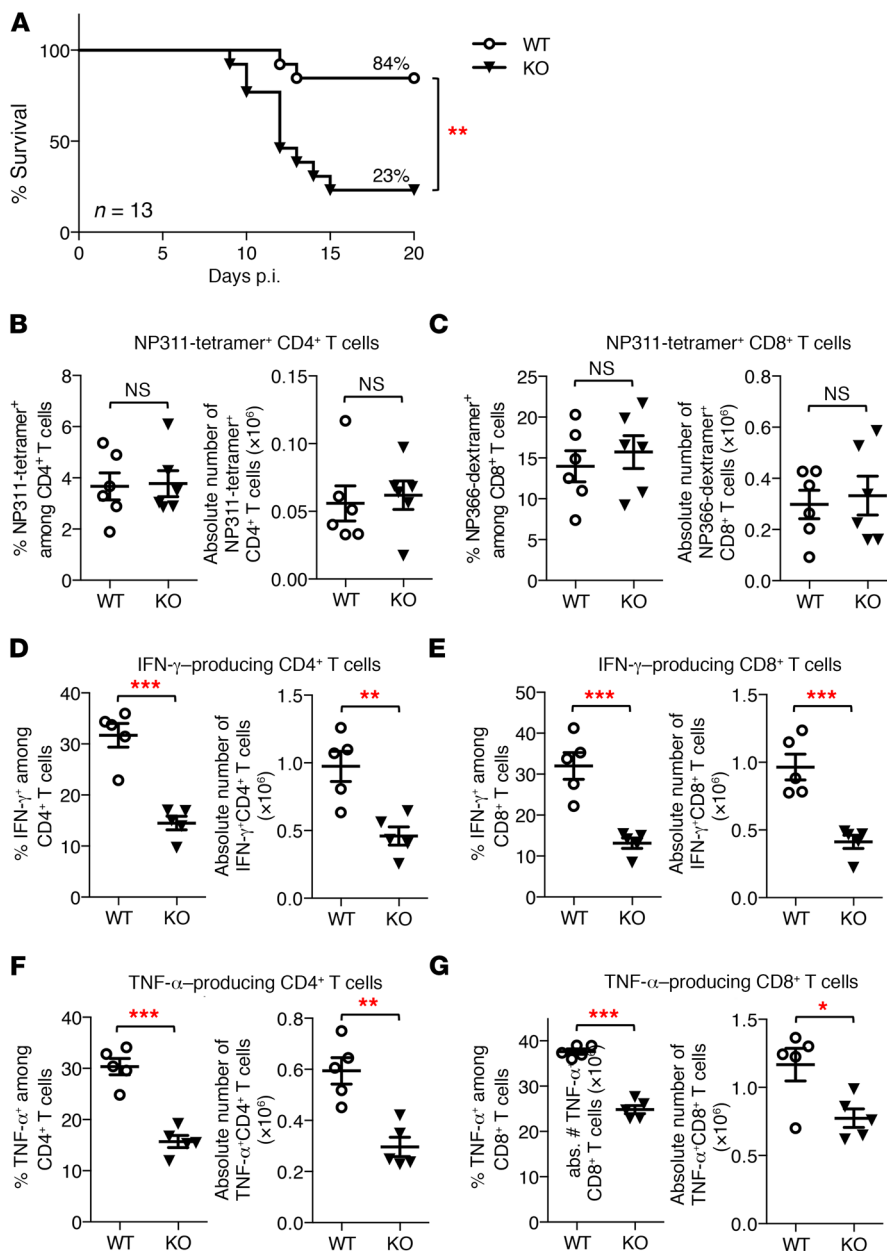
Figure 1. Toso deficiency results in increased mortality and reduced production of inflammatory cytokines by T cells upon influenza infection. WT and Toso^{-/-} (KO) mice were infected i.n. with 1,000 PFU influenza virus strain A/PR8 (H1N1). (**A**) Survival of mice was monitored over time. n = 13 per genotype; **P < 0.005; log-rank test. (**B** and **C**) Lung cells were isolated at day 9 p.i., and the frequency and number of virus-specific I-A[b]/NP$_{311-325}$ (NP311) tetramer–positive CD4+ T cells (**B**) and D[b]/NP$_{366-374}$ (NP366) dextramer–positive CD8+ T cells (**C**) were quantified. (**D**–**G**) Lung cells isolated on day 9 p.i. were restimulated ex vivo, and the number and frequency of IFN-γ–producing (**D** and **E**) and TNF-α–producing (**F** and **G**) CD4+ T cells (**D** and **F**) and CD8+ T cells (**E** and **G**) were quantified by intracellular cytokine staining. (**B**–**G**) Each symbol represents an individual mouse; horizontal lines indicate the mean ± SEM. (**B** and **C**) n = 6; (**D**–**G**) n = 5. *P < 0.05; **P < 0.01; ***P < 0.001; Student's t test. Data are representative of at least 4 independent experiments.

B cells in Toso[f/f]/CD19-Cre^{+/-} mice led to impaired production of TNF-α by CD4+ and CD8+ T cells, which was associated with significantly attenuated overall cecal pathology (mainly attributable to reduced tissue damage in the epithelium and the mucosa) and relative protection from weight loss compared with CD19-Cre^{+/-} control mice (Supplemental Figure 5).

Together, our data suggest that while expression of Toso on B cells is associated with enhanced protective T cell immunity during acute infection, it may also contribute to T cell–mediated immunopathological tissue damage under chronic inflammatory conditions.

Toso deficiency results in increased numbers of IL-10–producing B cells. The unexpected finding that T cell effector function is indirectly regulated by Toso expression on B cells prompted us to analyze functional characteristics of Toso-deficient B cells. Here, we first assessed the capacity of Toso^{-/-} B cells to produce

the antiinflammatory cytokine IL-10. To this end, purified B cells from WT and Toso^{-/-} mice were treated for 24 hours with BAFF, LPS, anti-CD40, or anti-IgM or were control treated. Most interestingly, Toso^{-/-} B cells exhibited a strongly increased capacity to produce IL-10 when compared with WT B cells (Figure 3A). Depending on the stimulus, splenic B cells from Toso^{-/-} mice induced up to 4-fold higher frequency and numbers of IL-10–producing cells (Figure 3, B and C). Increased production of IL-10 by B cells from Toso-deficient mice is a B cell–intrinsic phenotype, as it was specifically observed upon conditional deletion of Toso in B cells (Toso[f/f]/CD19-Cre^{+/-} mice), whereas B cells from Toso[f/f]/CD4-Cre^{+/-} mice and Toso[f/f]/CD11c-Cre^{+/-} mice exhibited normal IL-10 production (Figure 3, D and E). B cell cytokine production was, however, not generally affected by Toso deficiency, as activation-induced TNF-α production was normal in Toso^{-/-} B cells (Supplemental Figure 6).
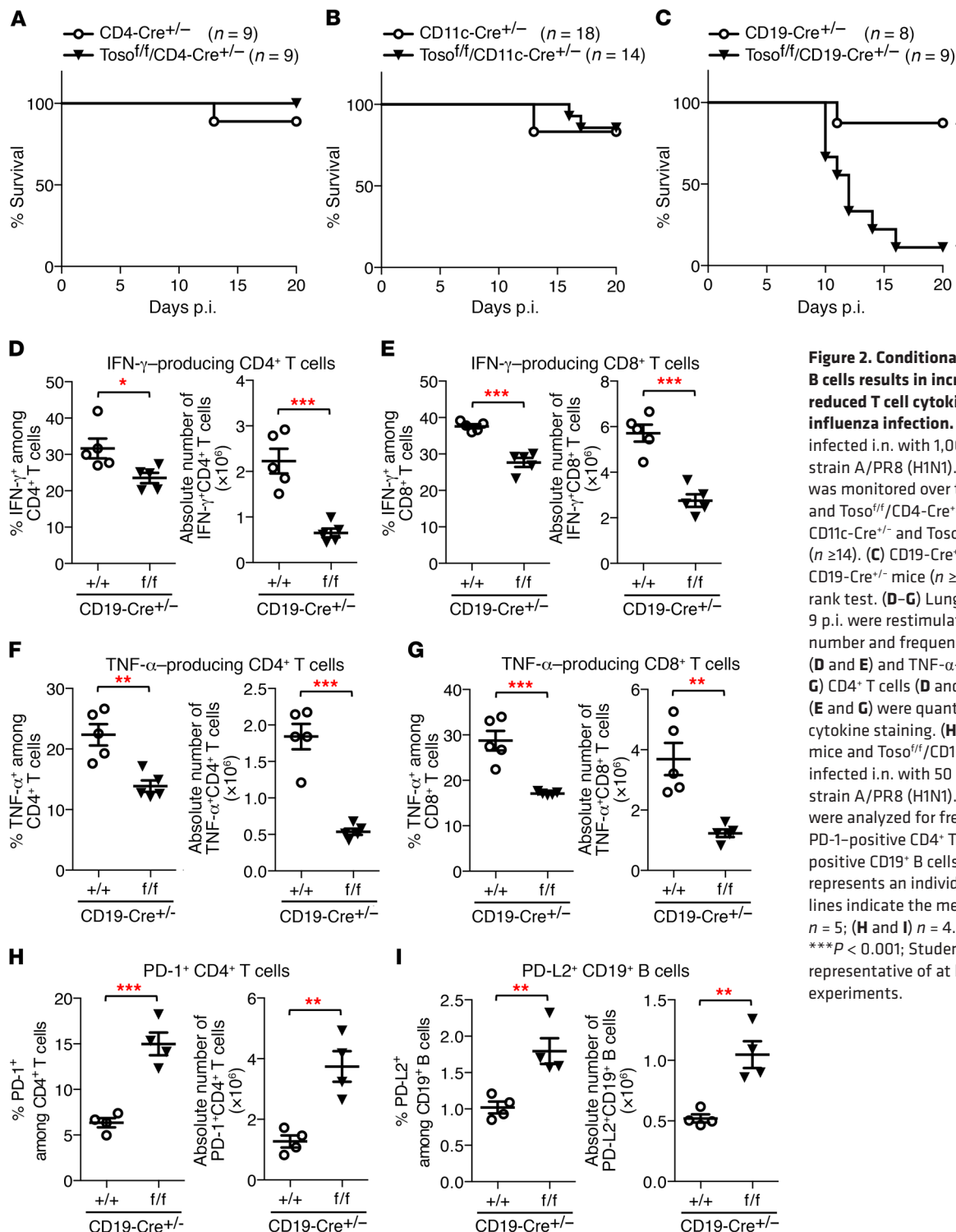
Figure 2. Conditional deletion of Toso in B cells results in increased mortality and reduced T cell cytokine responses upon influenza infection. (**A**–**G**) Mice were infected i.n. with 1,000 PFU influenza virus strain A/PR8 (H1N1). (**A**–**C**) Survival of mice was monitored over time. (**A**) CD4-Cre^{+/−} and Toso[f/f]/CD4-Cre^{+/−} mice (*n* = 9). (**B**) CD11c-Cre^{+/−} and Toso[f/f]/CD11c-Cre^{+/−} mice (*n* ≥14). (**C**) CD19-Cre^{+/−} mice and Toso[f/f]/CD19-Cre^{+/−} mice (*n* ≥8). **P* < 0.005; log-rank test. (**D**–**G**) Lung cells isolated on day 9 p.i. were restimulated ex vivo, and the number and frequency of IFN-γ–producing (**D** and **E**) and TNF-α–producing (**F** and **G**) CD4+ T cells (**D** and **F**) and CD8+ T cells (**E** and **G**) were quantified by intracellular cytokine staining. (**H** and **I**) CD19-Cre^{+/−} mice and Toso[f/f]/CD19-Cre^{+/−} mice were infected i.n. with 50 PFU influenza virus strain A/PR8 (H1N1). On day 7 p.i., spleens were analyzed for frequency and number of PD-1–positive CD4+ T cells (**H**) and PD-L2–positive CD19+ B cells (**I**). (**D**–**I**) Each symbol represents an individual mouse; horizontal lines indicate the mean (± SEM). (**D**–**G**) *n* = 5; (**H** and **I**) *n* = 4. **P* < 0.05; ***P* < 0.01; ****P* < 0.001; Student's *t* test. Data are representative of at least 3 independent experiments.

While only small numbers of IL-10–competent B cells are found in naive mice, number and frequency of IL-10–producing cells expand considerably upon influenza A infection (Figure 3, F and G). Importantly, also under these conditions of an in vivo viral infection, splenic B cells from Toso^{−/−} mice had a significantly higher capacity to produce IL-10, as compared with B cells from WT mice (Figure 3, F and G). Total B cell counts in the spleen and numbers of GL7+CD95+ germinal center B cells were similar between WT and Toso^{−/−} mice upon influenza A infection (Supplemental Figure 7). Finally, upon acute infection with influenza A virus, significantly higher frequency and numbers of IL-10–competent B cells were detected in the lungs of Toso[f/f]/CD19-Cre^{+/−} mice compared with CD19-Cre^{+/−} control mice (Figure 3H). Thus, taken together, our data suggest that Toso expression on B cells exhibits a B cell–intrinsic negative regulatory function on the capacity of these cells to produce the antiinflammatory cytokine
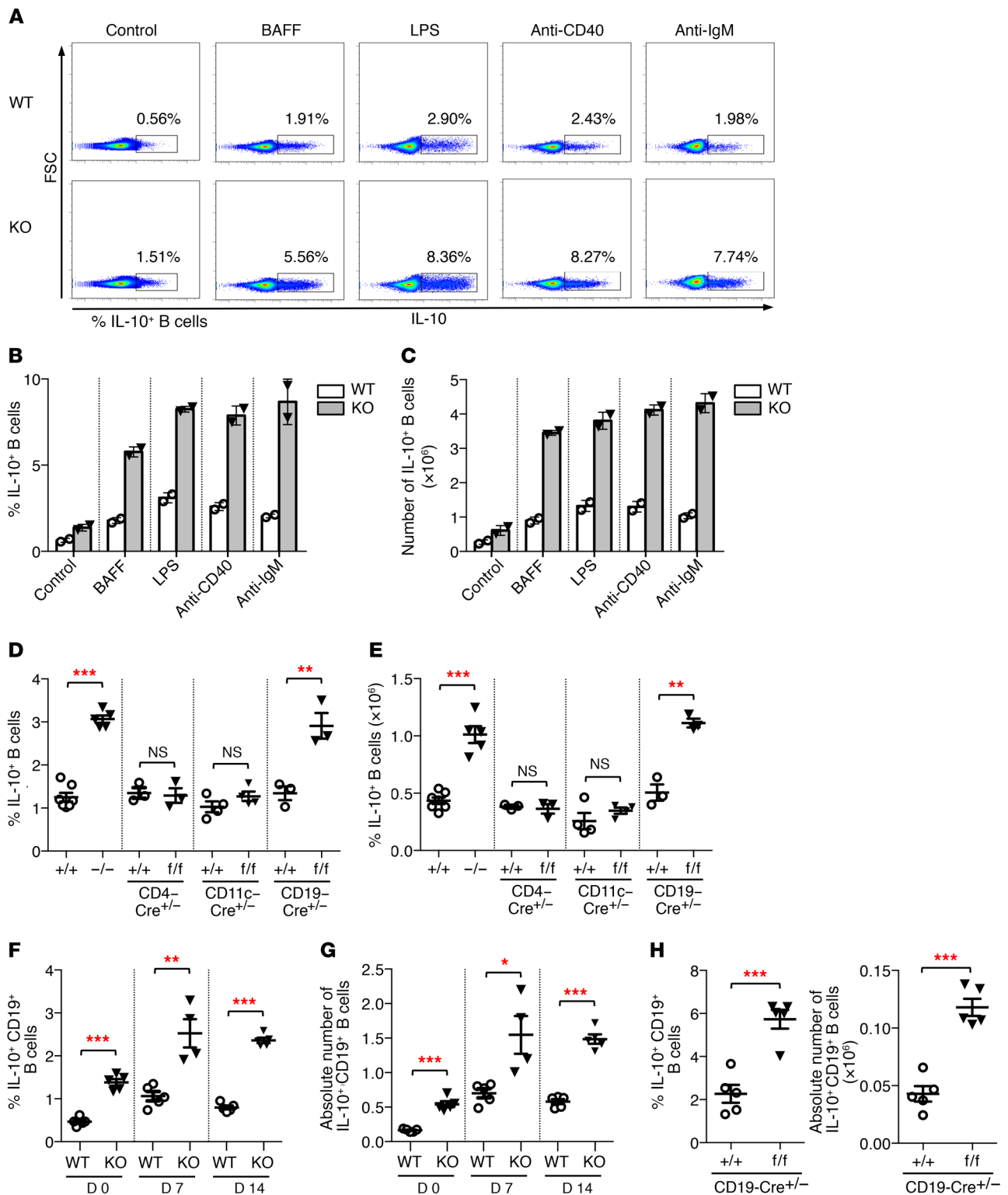
Figure 3. Toso deficiency results in increased numbers of IL-10–producing B cells. (**A**–**C**) Purified B cells from WT and Toso^{-/-} (KO) mice were treated with BAFF, LPS, αCD40, or αIgM for 24 hours. For the last 5 hours, cells were stimulated with PMA/ionomycin in the presence of brefeldin A (BFA)/monensin and subsequently analyzed for IL-10 production. (**A**) Representative flow cytometric analysis. (**B** and **C**) Bar graphs show frequency (**B**) and absolute numbers (**C**) of IL-10–positive B cells. Data are mean ± SEM from 2 cultures derived from different mice. (**D** and **E**) B cells from mice with straight and conditional Toso knockout, as well as the indicated control mice, were stimulated for 5 hours with LPS and PMA/ionomycin in the presence of BFA/monensin. Frequency (**D**) and number (**E**) of IL-10–positive B cells were determined by intracellular cytokine staining. (**F** and **G**) WT and Toso^{-/-} (KO) mice were infected i.n. with 50 PFU influenza virus strain A/PR8 (H1N1). At the indicated days p.i., splenocytes were restimulated ex vivo, and the frequency (**F**) and number (**G**) of IL-10–positive CD19^{+} B cells were quantified by intracellular cytokine staining. (**H**) CD19-Cre^{+/-} mice and Toso[f/f]/CD19-Cre^{+/-} mice were infected i.n. with 1,000 PFU influenza virus strain A/PR8 (H1N1). Lung cells isolated on day 9 p.i. were restimulated ex vivo, and number and frequency of IL-10–positive CD19^{+} B cells were quantified by intracellular cytokine staining. Each symbol represents an individual mouse; horizontal lines indicate the mean ± SEM. (**D** and **E**) $n = 3–7$; (**F**–**H**) $n = 4–5$. $*P < 0.05$; $**P < 0.01$; $***P < 0.001$; Student's t test. Data are representative of at least 3 independent experiments.

IL-10 both under steady-state conditions and in an inflammatory setting during viral infection.

Phenotypic characteristics of IL-10–competent B cell subsets. We next extended our analysis of IL-10–producing B cells onto different B cell subsets. Flow cytometric analysis of B cells from Vert-X IL-10 reporter mice — an IL-10-IRES-GFP knock-in mouse strain — showed that, upon LPS induction, essentially all splenic B1 cells (CD19^{+}B220^{lo}), as well as a small but significant fraction of B2 cells (CD19^{+}B220^{hi}), produced IL-10, as indicated by GFP expression (Supplemental Figure 8A). Thus, IL-10–competent B cell subsets reside within both B1 and B2 B cell compartments. IL-10–producing B1 cells exhibited a CD5^{hi} phenotype and showed low expression for CD1d, while, in line with previous reports (34), IL-10–producing B2 B cells were mainly characterized as CD1d^{hi}CD5^{int} cells. Importantly, intracellular IL-10 staining of activated WT and Toso^{-/-} B cells revealed that both of these IL-10–producing B cell populations — IL-10–producing B1a cells (B220[lo]) and IL-10–producing B2 cells (B220[hi]) — were markedly increased in B cell cultures from Toso^{-/-} mice, irrespective of whether IL-10 production was induced by treatment with BAFF/IL-21, LPS, or CpG oligonucleotides (Figure 4, A–C).

Based on B220 surface staining and the characteristic expression of CD1d on IL-10–producing B2 B cells, we were able to efficiently identify IL-10–competent B1 and B2 B cell subsets within untreated naive CD19^{+} B cells. High-purity cell sorting experiments showed that more than 90% of naive sorted B220^{lo} B1 cells could be induced to produce IL-10 (Figure 4, D and E). IL-10–competent B cells were also highly enriched within naive B220^{hi}CD1d^{+} B2 B cells, where approximately 50% of sorted cells could be induced to express IL-10 (Figure 4E). In contrast, the large population of B220^{hi}CD1d^{-} B2 B cells was largely unable to produce IL-10. We also examined whether IL-10–competent B220^{hi}CD1d^{+} B2 B cells are interrelated with B220^{hi}AA4.1^{+} transitional B2 cells; however, these two B2 B cell subsets were clearly distinct by CD1d versus AA4.1 surface expression (Figure 4F), and, importantly, IL-10 production could not be induced in B220[hi]AA4.1[+] transitional B cells (Figure 4G), thus also function-

ally confirming the different nature of these two different B cell subsets. Marginal zone (MZ) precursor B cells, which have been implicated in IL-10 production in a model of experimental arthritis (4), were also largely unable to produce IL-10 in our system (Supplemental Figure 8, B–E).

Further phenotypical analysis showed that the B220^{lo} B1 B cell population expresses high levels of CD5 and CD43, typical for B1a B cells, while IL-10–competent B220^{hi}CD1d^{+} B2 cells exhibit a CD5^{int}IgM^{hi}IgD^{lo}CD21^{hi}CD23^{lo} phenotype reminiscent of MZ B cells (Figure 4H and Supplemental Figure 8F). IL-10–incompetent B220^{hi}CD1d^{-} cells were mainly IgM^{lo}IgD^{hi}CD21^{int}CD23^{hi} follicular B cells (Figure 4H).

Detection of IL-10–producing B cells from influenza-infected mice required short-term ex vivo restimulation. Here, we observed that IL-10–producing B1 and B2 B cell subsets are substantially expanded in both lung and spleen from influenza A–infected mice compared with uninfected control mice (Supplemental Figure 9, A–C). Moreover, IL-10–producing B2 B cells (B2/IL-10 cells) from infected mice were also characterized by high expression of CD1d, and, under such an inflammatory context, IL-10–producing B1 and B2 B cells showed strong expression of Tim-1, CD73, and FasL (Supplemental Figure 9, D and E).

Most importantly, in Toso^{-/-} mice both of the IL-10–competent B cell subsets (B200^{hi}CD1d^{+} B2 cells and B220^{lo} B1a cells) were significantly increased in frequency and numbers (Figure 4I). Interestingly, however, on a per-cell basis, the cell-intrinsic capacity to produce IL-10 was comparable between the respective B cell subsets from WT and Toso^{-/-} mice (Figure 4E). Thus, Toso^{-/-} IL-10–competent B cells appeared to be functionally normal, but were present in significantly higher quantities upon genetic ablation of Toso.

Suppressive function of IL-10–producing Bregs. IL-10–producing B cells have been described as Bregs that exhibit immune regulatory functions and can downmodulate T cell responses and inflammatory reactions (35, 36). Thus, to demonstrate immunosuppressive activity of IL-10–producing B1 and B2 B cell subsets, we performed in vitro T cell–B cell coculture experiments. To this end, B cells from Vert-X IL-10/GFP reporter mice were purified by FACS into IL-10–producing B1 B cells (B220[lo]GFP[+]; "B1/IL-10 cells") and B2 B cells (B220[hi]GFP[+]; "B2/IL-10 cells"), as well as GFP-negative control B cells (B220^{hi}GFP^{-}; B2/effector cells). Sorted B cell populations were added to cultures containing purified naive CD4^{+} or CD8^{+} T cells. Cultures were stimulated with anti-CD3 mAbs, and proinflammatory cytokine production by CD4^{+} and CD8^{+} T cells was assessed. The frequency of IFN-γ^{+} and TNF-α^{+} CD8^{+} T cells was significantly reduced in cocultures with B1/IL-10 cells and B2/IL-10 cells, compared with cultures with B2/effector control cells (Figure 5, A and B). A similar suppressive effect of IL-10–producing B1 and B2 B cell subsets was observed in cocultures with naive CD4^{+} T cells (Figure 5C).

Next, we assessed whether freshly isolated naive B220^{lo} B1a cells and B220^{hi}CD1d^{+} B2 cells can also exhibit immunosuppressive function on T cell immunity. For these experiments on nonactivated B cell subsets, we performed adoptive transfer of purified naive B cell subsets followed by in vivo viral challenge. We adoptively transferred 1×10^6 FACS-sorted CD19^{+}B220^{lo} B1a cells, CD19^{+}B220^{hi}CD1d^{+} B2 B cells, and CD19^{+}B220^{hi}CD1d^{-} B2
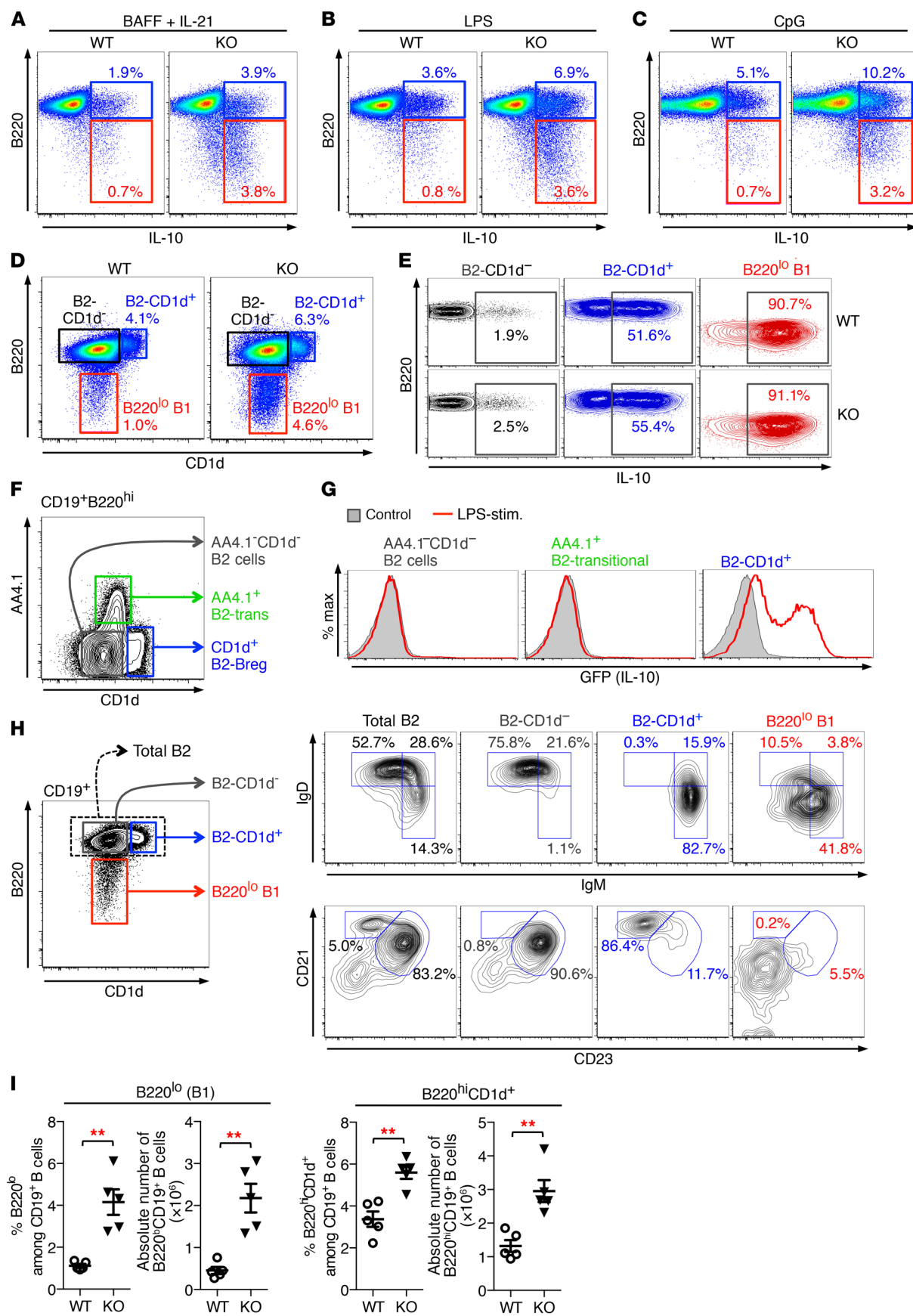
Figure 4. Phenotypic characteristics of IL-10–competent B cell subsets. (**A**–**C**) Purified B cells from WT and Toso$^{-/-}$ (KO) mice were cultured for 16 hours with BAFF plus IL-21 (**A**), LPS (**B**), or CpG oligonucleotides (**C**). For the last 5 hours, cells were treated with PMA/ionomycin in the presence of BFA/monensin and CD19$^+$ B cells analyzed for IL-10 production. (**D**) B220 versus CD1d staining on naive CD19$^+$ B cells from WT and Toso$^{-/-}$ (KO) mice. (**E**) B220^{hi} B2-CD1d$^-$ B cells (black), B220^{hi} B2-CD1d$^+$ B cells (blue), and B220^{lo} B1 B cells (red) from WT and Toso$^{-/-}$ (KO) mice were purified by FACS. Cells were stimulated for 16 hours with LPS plus PMA/ionomycin/BFA/monensin during the last 5 hours and subsequently analyzed for IL-10 production. (**F**) CD19$^+$B220^{hi} B cells were analyzed for CD1d versus AA4.1 (CD93) staining to identify AA4.1$^-$CD1d$^-$ B2-effector cells, AA4.1$^+$ transitional B2 cells (B2-trans), and CD1d$^+$ B2-Bregs. (**G**) AA4.1$^-$CD1d$^-$ B2-effector cells, AA4$^+$ B2-transitional cells, and CD1d$^+$ B2-Bregs were purified from IL-10/GFP reporter (Vert-X) mice by flow cytometric cell sorting. Cells were treated for 16 hours with LPS plus PMA/ionomycin during the last 5 hours and analyzed for GFP (IL-10) expression. (**H**) Flow cytometric analysis of naive B cells from C57BL/6J mice. Left panel is gated on CD19$^+$ B cells and shows gating for total B2 cells (B220^{hi}), B220^{hi}CD1d$^-$ B2 cells, B220^{hi}CD1d$^+$ B2 cells, and B220^{lo} B1 cells. FACS profiles on the right show expression of IgM versus IgD (top panel) and CD23 versus CD21 (bottom panel) on the indicated B cell subsets. (**I**) Number and frequency of splenic B220^{lo} B1 B cells and B220^{hi}CD1d$^+$ B2 cells in WT and Toso$^{-/-}$ (KO) mice. Each symbol represents an individual mouse; horizontal lines indicate the mean ± SEM. $n = 5$; **$P < 0.01$; Student's t test. Data are representative of at least 3 independent experiments.

B cells from untreated Toso$^{-/-}$ mice into C57BL/6 recipient mice. One day after adoptive transfer, mice were intranasally infected with influenza A, and cytokine responses in lung T cells were analyzed on day 9 p.i. (Figure 5D). In animals that had received CD19$^+$B220^{hi}CD1d$^-$ cells, virus-induced TNF-α or IFN-γ production by CD4$^+$ and CD8$^+$ T cells was comparable to that in normal control animals that had not received any transferred cells ("no transfer"; Figure 5, E–H). Adoptive transfer of naive CD19$^+$B220^{lo} B1a cells, however, had clear suppressive effects on virus-induced cytokine production by CD4$^+$ and CD8$^+$ T cells (Figure 5, E–H). Reduced TNF-α and IFN-γ production by T cells was also observed upon transfer of naive CD19$^+$B220^{hi}CD1d$^+$ B2 B cells, although its effects were less pronounced than those of CD19$^+$B220^{lo} B1a cells, consistent with the greater enrichment of IL-10 competency of CD19$^+$B220^{lo} B1a cells (Figure 4E). Based on their immunoregulatory function, CD19$^+$B220^{lo} B1a cells are here termed as "B1-Bregs" and CD19$^+$B220^{hi}CD1d$^+$ B2 cells as "B2-Bregs." Adoptively transferred naive B1- and B2-Bregs isolated from IL-10$^{-/-}$ mice did not exhibit measurable suppressive activity on proinflammatory cytokine production by CD4$^+$ and CD8$^+$ T cells during influenza A infection (Supplemental Figure 10), suggesting that IL-10 is a critical effector molecule of Bregs in vivo, although the involvement of alternative effector mechanisms, such as CD73-mediated adenosine generation, which has been reported to be affected in IL-10–deficient B cells (37), cannot be fully ruled out.

Our findings on adoptive transfer of as little as 1×10^6 cells demonstrate that naive B1-Bregs and B2-Bregs can both act as physiological regulators of T cell function by suppressing virus-induced T cell cytokine production during acute influenza A infection. Moreover, these data also provide a mechanistic explanation for the impaired T cell responses in Toso$^{-/-}$ mice during influenza A infection, which are likely caused by the higher numbers of immunosuppressive B1 and B2 Breg subsets in these mice.

B cell development in Toso-deficient mice. Toso surface expression is not restricted to B1 and B2 immunoregulatory B cells, but Toso is rather expressed on all peripheral B cells, with relatively highest expression on B220^{hi}CD1d$^-$ effector (follicular) B cells (Supplemental Figure 11A). Thus, how Toso specifically affects the generation of regulatory B cell subsets is still puzzling. Consistent with previous reports (24, 25) and the absence of Toso surface expression in early developmental B cell stages, we observed normal development of B cells in the bone marrow of Toso$^{-/-}$ mice (Supplemental Figure 11, B–G). Analysis of splenic B cells from Toso$^{-/-}$ mice revealed reduced frequency of mature IgM^{lo}IgD^{hi} B cells, while the population of IgM^{hi}IgD^{hi} transitional B cells was sig-

nificantly increased (Supplemental Figure 12, A and B). This was further accompanied by an increase in CD21^{hi}CD23^{lo} MZ B cells (Supplemental Figure 12, C and D), suggesting enhanced differentiation toward this particular B cell subset, which is also consistent with increased numbers of MZ-like B2-Bregs in Toso$^{-/-}$ mice.

In addition to slightly increased surface expression of IgM, we also noted that overall CD21 and CD23 expression levels, as well as CD62L surface levels, were slightly downregulated in Toso$^{-/-}$ B cells, further indicating alterations in peripheral B cell maturation/differentiation (Supplemental Figure 12, E–H). Expression of CD19, B220, IgD, MHC-II, and CD44 was not affected by Toso deficiency (Supplemental Figure 12H).

Furthermore, higher numbers of B220^{lo} B1a cells were found not only in the spleen of Toso$^{-/-}$ mice (Figure 4I and Supplemental Figure 13, A and B), but also in the peritoneal cavity, where an increase in B1a cells was accompanied by a corresponding decrease in B1b cells (Supplemental Figure 13, C and D). Analysis of peritoneal B cells revealed that B1a cells have an extremely high capacity to produce IL-10, whereas B1b cells are substantially less potent in IL-10 production (Supplemental Figure 13, E and F). Altogether, our analysis of B cell development in Toso$^{-/-}$ mice suggests that Toso is dispensable for B cell development in the BM, but fine-tunes the maturation/differentiation of specific B cell subsets in the periphery.

Self-reactivity of regulatory B cell subsets. Development of peripheral B cell compartments is tightly regulated, and even small changes in B cell maturation/differentiation may alter the balance of peripheral B cell tolerance. We thus next examined serum antibody levels and autoantibody production in Toso$^{-/-}$ mice. Basal levels of serum IgM and IgG were comparable between 8- to 10-month-old WT and Toso$^{-/-}$ mice (Figure 6A). However, consistent with published reports (21, 23–25), we detected elevated serum titers of autoreactive antibodies in Toso$^{-/-}$ mice. IgM and IgG antibodies directed against dsDNA or ssDNA were significantly increased in sera from aged Toso$^{-/-}$ mice compared with WT controls (Figure 6, B and C), supporting a role of Toso in the maintenance of self-tolerance.

To elucidate the major source of self-reactive antibodies in Toso$^{-/-}$ mice, we analyzed the capacity of different B cell subsets to produce autoantibodies. High-purity sorted B1- and B2-Bregs from Toso$^{-/-}$ mice exhibited strong production of anti-dsDNA and anti-ssDNA antibodies upon in vitro cultivation with LPS, while, in marked contrast, B2-effector cells and AA4.1$^+$ transitional B2 B cells were largely unable to produce self-reactive antibodies (Figure 6D). Efficient production of autoantibodies was not a specific feature of Toso$^{-/-}$ Bregs, but was similarly observed in WT B1- and
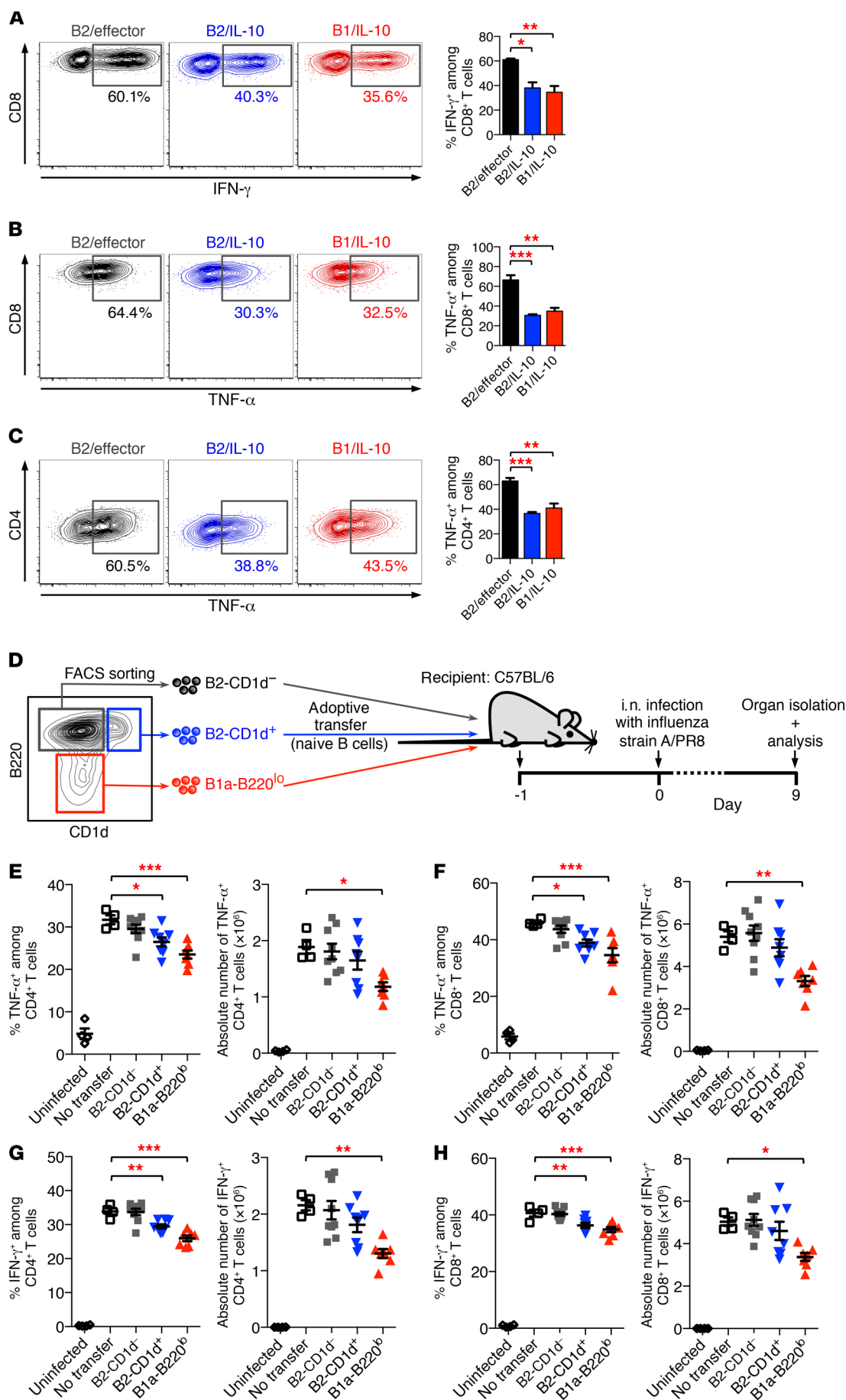
Figure 5. Suppressive function of IL-10–producing Bregs. (A–C) Bregs suppress inflammatory cytokine production in T cells in vitro. B cells from IL-10/GFP reporter (Vert-X) mice were treated for 16 hours with LPS, and PMA/ionomycin was added during the last 5 hours. B2/effector cells (B220^{hi}G-FP$^-$), B2/IL-10 cells (B220^{hi}GFP$^+$), and B1/IL-10 cells (B220^{lo}GFP$^+$) were then purified by FACS and were subsequently cocultured with naive CD8$^+$ T cells (**A** and **B**) or naive CD4$^+$ T cells (**C**). Cultures were stimulated with anti-CD3 for 48 hours and restimulated with PMA/ionomycin in the presence of BFA/monensin for 5 hours. Percentage of IFN-γ–producing (**A**) and TNF-α–producing (**B** and **C**) T cells was determined by intracellular cytokine staining. (**D–H**) Bregs suppress inflammatory cytokine production in T cells during antiviral immune response in vivo. (**D**) Experimental model. Briefly, naive CD19$^+$B220^{hi}CD1d$^-$ B2 B cells (gray), CD19$^+$B220^{hi}CD1d$^+$ B2 B cells (blue), and CD19$^+$B220^{lo} B1a cells (red) were purified from Toso$^{-/-}$ (KO) mice by FACS and were adoptively transferred into C57BL/6J mice. Mice were infected i.n. with 1,000 PFU influenza virus strain A/PR8 (H1N1). On day 9 p.i., lung cells were isolated and analyzed for cytokine staining. (**E–H**) Number and frequency of TNF-α–producing (**E** and **F**) and IFN-γ–producing (**G** and **H**) CD4$^+$ T cells (**E** and **G**) and CD8$^+$ T cells (**F** and **H**). Mice that had not received adoptively transferred cells (no transfer; open squares) but were also infected with influenza were used as positive control; uninfected mice served as a negative control (open circles). Data are expressed as mean ± SEM; symbols represent individual mice. (**A–C**) n = 3; (**E–H**) n = 4–9. *P < 0.05; **P < 0.01; ***P < 0.001; 1-way ANOVA and Dunnett's post hoc test. Data are representative of at least 3 independent experiments.

B2-Bregs (Supplemental Figure 14A). B2-effector cells and AA4.1$^+$ transitional B2 B cells exhibited only minimal autoantibody production under these conditions, even though they showed efficient blast formation and expression of the plasma cell marker CD138 (Supplemental Figure 14B). Together, these data indicate that self-reactive B cells are highly prevalent among B1-Bregs and B2-Bregs. Interestingly, IL-10–competent immunoregulatory B cell numbers rise as mice age, and increased numbers of Bregs in Toso$^{-/-}$ versus WT mice become even more pronounced in older mice (Figure 6, E and F). It is thus likely that the higher numbers of Bregs in Toso$^{-/-}$ mice are responsible for increased autoantibody levels in Toso$^{-/-}$ mice.

Toso fine-tunes B cell antigen receptor responsiveness. Regulation of B cell antigen receptor (BCR) signaling is a critical determinant of peripheral B cell differentiation/maintenance and the establishment of tolerance (38–41). We thus next evaluated the effects of Toso deficiency on BCR responsiveness and B cell activation/survival. Reflecting their different maturation/differentiation state, overall responsiveness to IgM receptor triggering varied considerably among different CD19$^+$ B cell subtypes. Upon anti-IgM stimulation, B2-effector cells (B220^{hi}AA4.1$^-$CD1d$^-$) proliferated vigorously, while B2-Bregs (B220^{hi}CD1d$^+$) and the IL-10–incompetent population of transitional B2 cells (B220^{hi}AA4.1$^+$), which both express high levels of IgM, rather showed induction of cell death. B1a B cells (B220^{lo}AA4.1$^-$CD1d$^-$; B1-Bregs) were largely unresponsive to anti-IgM triggering (Figure 6G and Supplemental Figure 15, A–E).

Toso$^{-/-}$ B2-effector cells showed a dose-dependent reduction in anti-IgM–induced cell proliferation, which was primarily associated with reduced cellular survival, while, similar to previous reports (25), the actual rate of cell divisions of live cells was comparable between WT and Toso$^{-/-}$ cells (Figure 6, H and I). Toso deficiency had, however, no effects on anti-IgM–induced survival/apoptosis of B1-Bregs, B2-Bregs, or B2-transitional cells (Supplemental Figure 15, A and B), and Toso$^{-/-}$ B cells also showed normal

survival upon treatment with other stimuli, such as LPS or BAFF plus IL-21 (Supplemental Figure 15, F and G).

As Toso interacts with the membrane BCR complex (22) and given the effects of Toso deficiency on B2-effector cell survival/proliferation, we examined the role of Toso in proximal BCR-mediated signaling events and early markers of B cell activation. Upon stimulation with anti-IgM, Toso-deficient B2-effector cells exhibited slightly impaired and less sustained phosphorylation of the tyrosine kinase Btk, indicating attenuated BCR signaling (Figure 6J). Lower Btk activation correlated with reduced induction of activation markers, such as CD25, CD69, and CD86, in Toso-deficient B cells (Figure 6, K and L, and Supplemental Figure 15H). It is noteworthy that IgM-mediated induction of activation markers was not fully impaired upon Toso deletion, but Toso$^{-/-}$ cells rather exhibited a relative shift in IgM receptor responsiveness (Figure 6L and Supplemental Figure 15H), indicating altered signaling/activation thresholds. Lower BCR-mediated induction of activation markers was also observed in Toso$^{-/-}$ B2-Bregs and B2-transitional cells, while, owing to their cell type–intrinsic low BCR responsiveness, B1-Bregs largely failed to respond to anti-IgM stimulation (Figure 6K). Together, these data indicate that Toso acts as a signal amplifier to fine-tune BCR responsiveness.

Anti-Toso treatment modulates IL-10–competent B cell numbers at sites of inflammation and results in impaired T cell responses upon influenza infection. Given the negative regulatory effect of Toso on IL-10–competent B cells and their immunosuppressive function on T cell immunity, we sought to investigate the effects of anti-Toso antibody treatment on B and T cell responses in the influenza-induced lung inflammation model and to evaluate its potential for immunomodulatory therapeutic applications. To induce virus-mediated lung inflammation, mice were infected intranasally with influenza A. One day before infection and on days 2 and 5 p.i., mice were treated with either anti-Toso mAb or control IgG, and B cells in inflamed lungs were analyzed on day 9 p.i. Notably, Toso is highly expressed on essentially all peripheral B cells; however, in vivo anti-Toso mAb application did not result in B cell depletion, as comparable numbers of B cells were detected in lungs of anti-Toso and control IgG–treated mice (Figure 7A). Treatment with anti-Toso mAb did, however, induce a striking increase in both frequency and absolute numbers of IL-10–competent B cells in lungs from influenza-infected animals (Figure 7B). Importantly, consistent with our findings on Toso-deficient mice, increased numbers of IL-10–competent B cells correlated with impaired T cell responses at sites of inflammation, as virus-induced TNF-α and IFN-γ production by CD4$^+$ and CD8$^+$ T cells was significantly reduced in lungs of mice that had received Toso mAb compared with control IgG–treated mice (Figure 7, C–F). Together, these data re-emphasize the immunoregulatory role of Toso during inflammatory disease. Furthermore, as Toso is conserved between mice and humans and is also expressed on human B cells (ref. 19 and Supplemental Figure 16), the data also suggest that Toso may provide a promising therapeutic target to modulate IL-10–competent B cell compartments and to dampen excessive T cell responses at local sites of inflammation.

Discussion

Using conditional gene deletion, we here demonstrate that impaired antiviral T cell responses upon influenza A infection in
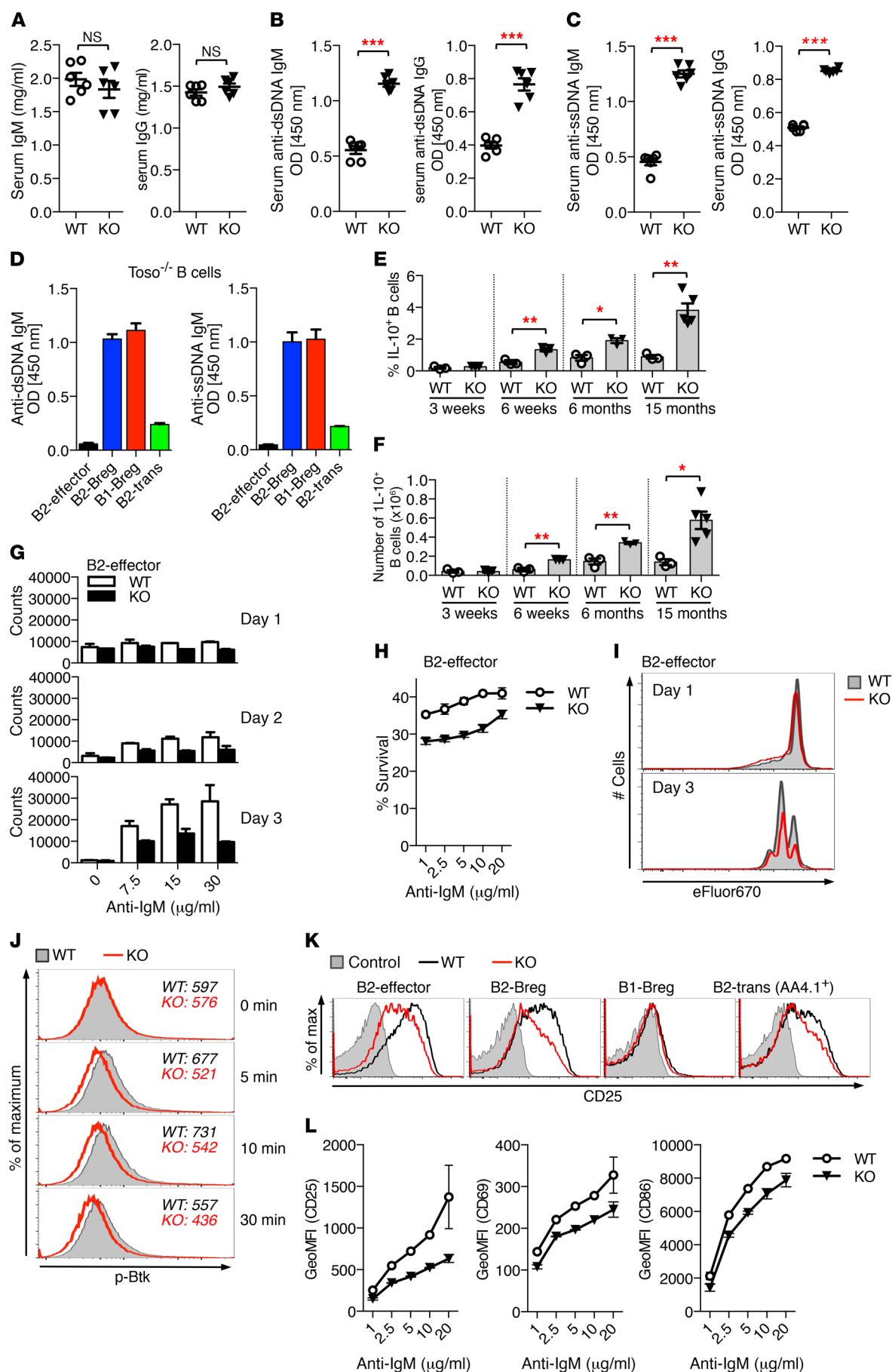
Figure 6. Self-reactivity of regulatory B cell subsets and altered activation thresholds of Toso-deficient B cells. (**A**–**C**) Serum from 8- to 10-month-old female WT and Toso$^{-/-}$ (KO) mice was analyzed for total IgM and IgG levels (**A**) and titers of IgM and IgG antibodies against dsDNA (**B**) and ssDNA (**C**). *n* = 6. (**D**) Sorted B220^{hi}AA4.1$^-$CD1d$^-$ B2-effector cells, B220^{hi}CD1d$^+$ B2-Bregs, B220hiAA4.1$^+$ B2-transitional cells (B2-trans), and B220lo B1-Bregs from Toso$^{-/-}$ mice were treated for 3 days with LPS. Culture supernatants were analyzed for anti-dsDNA and anti-ssDNA IgM levels (*n* = 2). (**E** and **F**) Frequency (**E**) and numbers (**F**) of IL-10–positive splenic B cells from WT and Toso$^{-/-}$ mice of the indicated ages. *n* = 3–5. (**G** and **H**) Sorted B2-effector cells from WT and Toso$^{-/-}$ (KO) mice were stimulated for the indicated durations with titrated amounts of anti-IgM and analyzed for cell counts (*n* = 2) (**G**) and cell survival (*n* = 4) (**H**). (**I**) Sorted B2-effector cells were labeled with eFluor670, stimulated with anti-IgM, and analyzed for cell division. (**J**) Sorted B2-effector cells from WT (gray filled) and Toso$^{-/-}$ (KO) (red line) mice were stimulated for the indicated durations with anti-IgM and analyzed for phospho-Btk (p-Btk) staining. (**K** and **L**) Sorted B cell subsets were stimulated for 16 hours with anti-IgM and analyzed for B cell activation markers. (**K**) Representative flow cytometric histograms for CD25 expression. WT, black; Toso$^{-/-}$ (KO), red line; unstimulated control, gray filled. (**L**) Sorted B2-effector cells were analyzed for anti-IgM–induced upregulation of CD25, CD69, and CD86. Data show the geometric mean fluorescence intensity (GeoMFI) (*n* = 2). Data are expressed as the mean ± SEM. *P < 0.05; **P < 0.01; ***P < 0.001; Student's *t* test. All data are representative of 2 to 4 independent experiments.

Toso$^{-/-}$ mice were not due to T cell–inherent defects, but rather were induced by a previously unrecognized role of Toso in B cells. Our findings thus reveal an unexpected regulatory activity of B cells on T cell function during viral infection. Deletion of Toso on B cells results in a strong increase of IL-10–competent B cells, and, as we further demonstrate, this specific subtype of B cells mediates immunosuppressive activity on T cell responses during viral infection, most likely via an IL-10–dependent mechanism. Immunosuppressive function of IL-10 during influenza infection has been demonstrated in studies on IL-10$^{-/-}$ mice (42, 43). Moreover, B cells have been shown to be a relevant source of IL-10 during viral infection (44). B cells upregulate IL-10 expression during infection with murine cytomegalovirus, and this B cell–derived IL-10 decreases virus-specific IFN-γ responses in CD8$^+$ T cells (44). Considering our data, we thus propose that Toso promotes efficient antiviral T cell cytokine responses by restricting the size of the IL-10–competent B cell pool. Specifically, B cell–intrinsic expression of Toso restricted differentiation/maintenance of IL-10–competent B cells in vivo. At the cellular level, Toso$^{-/-}$ Bregs exhibited normal functions. Hence, the impaired T cell responses observed in Toso$^{-/-}$ mice following influenza infection likely reflect the increased numbers of Bregs in Toso-deficient mice.

The present study demonstrates that IL-10–competent B cells are highly enriched within 2 distinct subpopulations of B cells, the small fraction of splenic B220^{hi}CD1d$^+$CD5^{int} B2 cells and the fraction of B220^{lo}CD5^{hi} B1a cells. These findings are consistent with earlier descriptions of B1a B cells as highly potent producers of IL-10 (45) and recent reports of an IL-10–competent population of CD19^{hi}CD1d$^+$CD5$^+$ B cells, termed B10 cells, that exhibits immunoregulatory function in models of autoimmunity (6, 8, 34, 46). Interestingly, IL-10–competent B220^{hi}CD1d$^+$CD5^{int} B cells share many surface marker characteristics with MZ B cells.

Adoptive transfer of naive B cell subsets showed that both major IL-10–competent B cell compartments — B220^{hi}CD1d$^+$

CD5^{int} B2 cells (B2-Bregs) and B220^{lo}CD5^{hi} B1a cells (B1-Bregs) — exhibit immunosuppressive activity on influenza-induced T cell responses. Adoptively transferred Bregs from IL-10–deficient mice did not exhibit such potent suppressive activity on T cell cytokine production, suggesting that the immunoregulatory function of Bregs is largely mediated via IL-10. It is, however, conceivable that, depending on the specific inflammatory context, additional mechanisms, such as PD-L2/PD-1, CD80/CTLA4, GITR/GITRL, or FasL/Fas interactions, secretion of TGF-β or IL-35, or CD73-mediated adenosine generation, also contribute to the inhibitory function of B1- and B2-Bregs (37, 47–51).

An important but largely unexplored aspect of Bregs is their antigen specificity. We here show that IL-10–competent B1- and B2-Bregs exhibit a high prevalence of autoreactivity and readily secrete self-reactive antibodies upon TLR stimulation. Self-reactivity is a typical feature of B1a and MZ B cells, which express polyreactive BCRs that can bind both to pathogens and to self-antigens (52). Considering this and the striking similarities in surface marker characteristics between regulatory B cell subsets and B1a/MZ B cells, it is thus an intriguing idea that the majority of Bregs originate from B1a and MZ B cells and/or their precursors — the reported phenotypic diversity of Bregs may be more related to effects of the specific inflammatory milieu and particular tissue environment and/or reflect differences in the cellular activation status. Supporting evidence for this idea comes from earlier studies that have characterized B1 and MZ B cells as major IL-10–producing B cells and have demonstrated regulatory function of these specific B cell subsets in different models of inflammatory disorders and autoimmunity (45, 53–59). Consistent with Bregs being closely related to B1a and MZ B cells, the observed increase in IL-10–competent B cells in Toso$^{-/-}$ mice correlated with a corresponding increase in B1a and MZ B cells. While an increase in B1a cells has also been observed in other Toso-deficient mouse strains, MZ B cell numbers were reported to be either decreased or unchanged (21, 23, 24). Discrepancies in MZ B cell numbers may be due to different targeting strategies and use of different embryonic stem cell lines (129/Sv vs. B6) and also be related to slightly altered expression levels of CD21 and CD23 in Toso$^{-/-}$ B cells, which complicate MZ B cell identification. Given their potential to produce self-reactive antibodies, increased numbers of B1a and MZ B cells likely also account for the elevated, albeit nonpathogenic, levels of IgM and IgG autoantibodies that we and others have detected in Toso$^{-/-}$ mice (21, 23–25). In the NZB/W mouse model of systemic lupus erythematosus, B1 and MZ B cells are also expanded and spontaneously secrete IgM autoantibodies and can produce self-reactive, isotype-switched IgG antibodies (60, 61). Consistent with a regulatory capacity of B1a and MZ B cells, the number of IL-10–producing B cells was also found to be increased in young NZB/W mice prior to disease onset (62).

Altogether, these findings suggest that, in analogy to natural regulatory T cells (1), Bregs are characterized by self-reactive antigen receptors and, upon appropriate activation, utilize the secretion of immunomodulatory cytokines, such as IL-10, as a major effector mechanism to prevent excessive inflammatory reactions. Our observation that IL-10–producing B cells expand in numbers and are recruited to the site of inflammation during influenza-induced pulmonary disease thus suggests a scenario in which recognition of self-antigens (which are exposed as a result of tissue
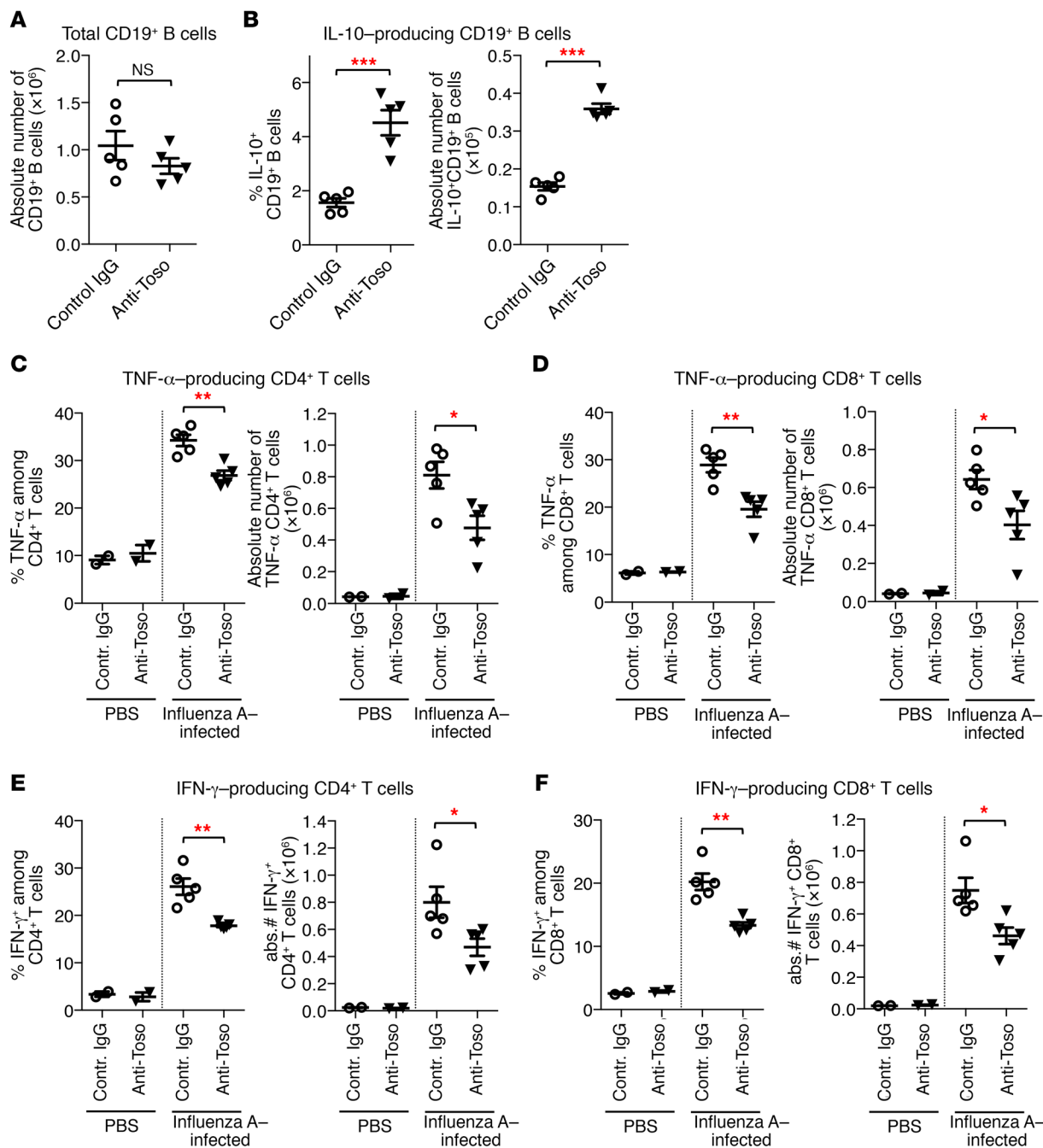
Figure 7. Immunomodulatory effect of Toso-blocking antibody treatment on influenza-induced lung inflammation. Mice were infected i.n. with influenza virus strain A/PR8 (H1N1) to induce pulmonary inflammation. On day –1, day 2, and day 5 p.i., mice were treated with anti-Toso mAb or control IgG (200 μg/mouse; i.v.). Lung cells isolated on day 9 p.i. were restimulated ex vivo and analyzed for cytokine production in T and B cells by intracellular cytokine staining. (**A**–**C**) Quantification of total CD19+ B cells (**A**) and frequency (**B**) and number (**C**) of IL-10–positive B cells in lungs of infected animals. (**C**–**F**) Quantification of frequency and numbers of TNF-α–producing (**C** and **D**) and IFN-γ–producing (**E** and **F**) CD4+ T cells (**C** and **E**) and CD8+ T cells (**D** and **F**). (**A**–**F**) Each symbol represents an individual mouse; horizontal lines indicate the mean ± SEM. PBS control, $n = 2$; influenza A–infected mice, $n = 5$. *$P < 0.05$; **$P < 0.01$; ***$P < 0.001$; Student's t test. Data are representative of 2 independent experiments.

damage) by autoreactive Bregs induces their immunosuppressive activity to dampen the inflammatory response and limit immunopathology. We thus propose that the population of Bregs is normally tightly controlled, to ensure a well-balanced immune response that allows for efficient immune protection against pathogens while minimizing immunopathological tissue damage. Mice with Toso

deficiency on B cells have increased numbers of Bregs and, thus, a "dysregulated" system, which results in impaired ("suppressed") proinflammatory T cell responses (see model in Supplemental Figure 17). Our data indicate that during acute influenza infection, in which antiviral immune protection is largely dependent on effector T cells, such suppressed T cell responses are detrimental and are

associated with impaired immune protection and an increased risk of mortality. In contrast, under chronic inflammatory conditions, such as the chronic bacterial-induced model of colitis, in which effector T cells are more associated with immunopathological tissue damage, higher numbers of Bregs and, thus, impaired T cell effector function are beneficial, as this limits T cell–mediated tissue destruction (Supplemental Figure 17).

Differentiation and homeostasis of peripheral B cell subsets is critically influenced by signaling through the BCR (38–41). In line with altered peripheral B cell compartments in Toso-deficient mice, we here demonstrate that Toso shifts the threshold for BCR-mediated cellular activation/survival pathways. The exact molecular mechanism of how Toso affects BCR responsiveness is currently unknown. As an IgM-binding molecule, Toso may interact directly with membrane-bound IgM-containing BCR complexes (22) or, alternatively, may indirectly affect B cell signaling via recognition of soluble IgM immune complexes. Increased tonic signaling in Toso-deficient B cells (21) could not be confirmed in our study and may be related to the unusual occurrence of a lymphoproliferative disorder in this particular strain of mice, which has not been observed in any other strain of Toso-deficient mice.

Infection with influenza virus is frequently associated with severe pulmonary immune pathology in human patients. The anatomical structures in the lung are highly sensitive to tissue destruction, necessitating a fine balance between pro- and anti-inflammatory responses during pulmonary infection. In particular, after viral clearance, excessive release of proinflammatory cytokines by continually recruited $CD8^+$ T cells can cause severe lung tissue injury. In the present study, we show that during influenza A–induced pulmonary inflammation the application of Toso blocking antibody selectively induces IL-10–competent B cells at the site of inflammation, an effect that was associated with reduced production of proinflammatory cytokines by lung T cells. These data suggest that clinical targeting of Toso may provide a novel therapeutic approach to control pathogenic T cell responses via the modulation of IL-10–competent B cell compartments at local sites of inflammation.

Methods

Mice and viral infection. Mice with constitutive Toso knockout (Toso$^{-/-}$) and the generation of mice with a conditional floxed Toso allele (Toso$^{f/f}$ mice) have been described before (18). In brief, the targeting vector was designed to have exons 4–7 flanked by loxP sites. After transfection into C57BL/6 embryonic stem cells, targeted embryonic stem cell clones were identified by Southern blotting and were injected into blastocysts. Upon germline transmission the frt-flanked neomycin-selection cassette was removed by breeding with C57BL/6 flp deleter mice. The resulting floxed-targeted mouse lines were crossed with the EIIa-Cre transgenic mouse line (http://www.informatics.jax.org/reference/J:70555) to obtain Cre-mediated total germline excision of exons 4–7 (constitutive Toso knockout). Toso-deficient and Toso-floxed mice were backcrossed for more than 8 generations with C57BL/6J. To obtain cell type–specific conditional deletion, Toso-floxed (Toso$^{f/f}$) were crossed with transgenic mouse lines expressing Cre-recombinase under control of the *cd4* promoter [CD4-Cre mice: Tg(Cd4-cre)1Cwi] (http://www.informatics.jax.org/reference/J:73127), the *cd11c* (*Itgax*) promoter [CD11c-Cre mice: Tg(Itgax-cre,-EGFP)4097Ach] (http://www.

informatics.jax.org/reference/J:123556), or the *cd19* promoter [CD19-Cre mice: Cd19$^{tm1(cre)Cgn}$] (http://www.informatics.jax.org/reference/J:67676). Vert-X IL-10 reporter mice [B6(Cg)-Il10$^{tm1.1Karp}$] (http://www.informatics.jax.org/reference/J:151551) that carry an internal ribosome entry site (IRES)–enhanced green fluorescent protein (eGFP) fusion protein downstream of exon 5 of the interleukin-10 (Il10) gene were used for some experiments. Cre-expressing transgenic mouse lines, IL-10 reporter mice, and IL-10–deficient mice (B6.129P2-Il10^{tm1Cgn}; http://www.informatics.jax.org/allele/MGI:1857199; provided by A. Bleich and I. Brüsch, Hannover Medical School) were all on C57BL/6J background and were originally obtained from The Jackson Laboratory. Mice were housed in individually ventilated cages under specific pathogen–free conditions in the barrier animal facility at Hannover Medical School. Mice were infected at 10–13 weeks of age. Controls were sex- and age-matched. For in vivo influenza infection, mice were anesthetized with ketamine-xylazine. Virus was diluted in sterile PBS, and mice were infected by intranasal (i.n.) administration of a total volume of 40 μl of PR8 influenza virus. Mice were monitored daily for weight loss, signs of illness, and survival. Anti-Toso mAb or control rat IgG (catalog 012-000-003, Jackson ImmunoResearch) was administered i.v. on days –1, 2, and 5 p.i. (200 μg/mouse/time point). To examine the primary immune response, cells were harvested from lungs and spleen on the indicated days postinfection. Bronchoalveolar lavage fluid was collected for viral titer measurements.

Salmonella infection studies. Streptomycin (20 mg/mouse) was given by oral gavage to mice aged 16 weeks. Twenty-four hours after antibiotic administration, mice were infected with *Salmonella* Typhimurium Δ*aroA* at a dose of 3×10^6 bacteria in 100 μl HEPES buffer (100 mM, pH 8.0). Control mice (mock infection) were given 100 μl HEPES buffer. For histopathological analysis, tissues were fixed in 10% neutral buffered formalin overnight and embedded in paraffin. Cecum sections (5 μm) were deparaffinized and stained with H&E. Histological scores in the ceca of infected mice were determined as previously described (63). Briefly, pathological changes were assessed by evaluation of various parameters such as presence of luminal cells, infiltrating immune cells, crypt abscesses, and the formation of edema in the respective layer of the intestinal bowel wall including the surface epithelium, mucosa, and submucosa.

Influenza virus. Influenza virus strain A/PR8 (A/Puerto Rico/8/34 [H1N1]) was obtained from ATCC. Virus was grown in Madin-Darby canine kidney (MDCK) cells (obtained from ATCC). Viral titers were determined by standard MDCK plaque titration assay. Briefly, serial 10-fold dilutions of virus stock or bronchoalveolar lavage fluid from infected mice were allowed to adsorb onto 90% confluent MDCK cells on a 24-well plate. After 2.5 hours of incubation, cells were overlaid with 1.2% Avicel RC-581 (IMDC Deutschland GmbH) in DMEM (Gibco) supplemented with 0.1% BSA, 1% L-glutamine, penicillin, streptomycin, and 1 μg/ml TPCK Trypsin (Thermo Fisher Scientific) and cultured for 24 hours at 37°C in 5% CO_2. Cells were washed, fixed, and permeabilized, and virus plaques were visualized and enumerated by staining with an mAb against influenza A nucleoprotein (AA5H, AbD Serotec). Viral titers were calculated as PFU per milliliter.

Flow cytometry (FACS). Single-cell suspensions of spleen, bone marrow, and peritoneum were prepared from fresh tissue using standard procedures. To isolate pulmonary lymphocytes, lung lobes were minced and strained through nylon mesh. Following red blood cell lysis, cells were blocked with anti-CD16/32 (clone 93, Biolegend) and

subsequently stained with fluorescent-labeled mAbs summarized in Supplemental Table 1. Anti-Toso mAb (rat IgG2a) directed against the extracellular domain of murine Toso was generated by DNA vaccination (18) and was directly conjugated with DyLight 649 (Thermo Fisher Scientific). APC-labeled MHC-II I-A^b/NP$_{311-325}$ (NP311) tetramer (containing QVYSLIRPNENPAHK of influenza virus nucleoprotein) was obtained from the NIH Tetramer Core Facility (Emory University Vaccine Center, Atlanta, Georgia, USA), and APC-labeled D^b/NP$_{366-374}$ (NP366) dextramer (containing ASNENMETM of influenza virus nucleoprotein) was purchased from Immudex. For discrimination of live versus dead cells, we used the fixable viability dye eFluor450 (eBioscience). For the detection of intracellular cytokines, cells were restimulated ex vivo in the presence of brefeldin A and monensin (both eBioscience). After cell surface staining, cells were fixed with paraformaldehyde and permeabilized using Perm/Wash buffer (eBioscience) and stained with mAbs against TNF-α (MP6-XT22), IFN-γ (XMG1.2), or IL-10 (JES5-16E3; all Biolegend). Flow cytometric measurements were performed on a FACSCanto II cell analyzer (BD Biosciences). Data were analyzed with FlowJo software (version 9.9.3, Mac; version 10.0.7, PC; Tree Star).

Cell sorting and adoptive transfer experiments. For high-purity cell sorting experiments, splenic B cells were first enriched by magnetic isolation using negative selection (pan–B cell isolation kit; Miltenyi Biotec and Stemcell Technologies). B cell subpopulations were then further purified following immunofluorescence surface staining using high-speed flow cytometry cell sorters (FACSAria Fusion and FACSAria IIu, both BD Biosciences). To obtain highly pure B cell subsets with minimal contamination by other cell types, we pre-gated on viable cells that were CD19$^+$, but negative for CD4, CD8, F4/80, and NK1.1. Further gating of B cell subsets was primarily based on B220, CD1d, and AA4.1 surface expression or B220 versus GFP (IL-10) expression. Sorted B cell subsets had greater than 98% purity.

For adoptive transfer experiments, FACS-sorted B cell subsets were immediately transferred i.v. into syngeneic C57BL/6J recipient mice (1 × 10^6 cells per recipient mouse). One day after adoptive transfer, mice were infected i.n. with influenza virus strain A/PR8. On day 9 p.i., lung cells were isolated, restimulated ex vivo, and subjected to flow cytometric analysis.

Ex vivo cell restimulation, cell activation, and B cell cultures. For the detection of T cell cytokine production, cells were restimulated ex vivo for 5 hours in the presence of brefeldin A and monensin (both eBioscience) on tissue culture plates that had been precoated with anti-CD3 (10 μg/ml; clone 145-2C11, eBioscience) and anti-CD28 (2 μg/ml; clone 37.51, Biolegend). Where indicated, splenocytes were restimulated for 6 hours with influenza A virus peptide of amino acids 366–374 of the viral nucleoprotein (NP366 peptide), an H-2K^b–restricted epitope that is specific for CD8$^+$ T cells, in the presence of brefeldin A and monensin. To assess IL-10 production by B cells during influenza A virus infection, cells were restimulated ex vivo for 5 hours with PMA (50 ng/ml; Sigma-Aldrich) and ionomycin (500 ng/ml; Sigma-Aldrich) in the presence of brefeldin A and monensin. Following ex vivo restimulation, cells were subjected to cell surface and intracellular FACS staining.

For the in vitro analysis of IL-10 production by B cells, isolated leukocytes or purified B cell populations were cultured for the indicated times with ultrapure LPS (500 ng/ml; InvivoGen), CpG oligonucleotides (10 μg/ml; InvivoGen), BAFF (200 ng/ml; Biolegend), anti-

CD40 (10 μg/ml; clone 1C10, Biolegend), anti-IgM [10 μg/ml; goat anti–mouse F(ab′)$_2$ fragment, Jackson ImmunoResearch], or a combination of BAFF (200 ng/ml) plus IL-21 (50 ng/ml; Biolegend). PMA (50 ng/ml; Sigma-Aldrich) and ionomycin (500 ng/ml; Sigma-Aldrich) plus brefeldin A and monensin (both eBioscience) were added during the last 5 hours of culture. Cells were subsequently analyzed by intracellular flow cytometry.

For some experiments, FACS-sorted B cell populations were stimulated for the indicated times with titrated amounts of anti-IgM [goat anti–mouse F(ab′)$_2$ fragment, Jackson ImmunoResearch], and cultures were subsequently analyzed by flow cytometry for cell survival and upregulation of activation markers. To analyze in vitro autoantibody production, FACS-sorted B cell populations were stimulated for 3 days as indicated. Culture supernatants were then collected for the detection of autoantibodies, and cells were analyzed by flow cytometry.

For the analysis of B cell signaling, FACS-sorted B effector cells were stimulated with anti-IgM [10 μg/ml; goat anti–mouse F(ab′)$_2$ fragment, Jackson ImmunoResearch]. Stimulation was stopped by fixation in paraformaldehyde. Cells were then permeabilized using Perm/Wash buffer (eBioscience), stained with anti–phospho-Btk/Itk (Tyr551, Tyr511; eBioscience), and analyzed by flow cytometry.

ELISA and detection of autoantibodies. Serum titers of IgM and IgG were determined by specific ELISA kits (eBioscience) according to the manufacturer's protocol. To detect autoantibodies in serum and cell culture supernatants, high-binding ELISA plates (Greiner) were coated overnight with 2 μg/ml ssDNA or dsDNA from calf thymus (Sigma-Aldrich). ssDNA was obtained by heat denaturation of dsDNA (95°C, 10 minutes) followed by rapid cooling on ice. Coated plates were blocked with 1% BSA, 0.5% gelatin in TBS for 2 hours at room temperature, and diluted samples were incubated overnight at 4°C in TBS 1% BSA. Bound anti-ssDNA or anti-dsDNA antibodies were detected with HRP-conjugated anti-mouse IgG (eBioscience) or with anti-mouse IgM-biotin (Jackson ImmunoResearch) and streptavidin-HRP (R&D Systems) followed by TMB substrate solution (eBioscience). Absorbance was measured at 450 nm.

In vitro B cell suppression assay. Splenic B cells from Vert-X IL-10 reporter mice were isolated by positive selection using CD19-coupled MicroBeads (Miltenyi Biotec) and were cultured for 16 hours with ultrapure LPS (500 ng/ml) plus addition of PMA (50 ng/ml) and ionomycin (500 ng/ml) during the last 5 hours. B cell cultures were surface-stained, and indicated CD19$^+$ B subpopulations were purified with greater than 98% purities by FACS based on B220 versus GFP (IL-10) expression. Naive CD4$^+$ and naive CD8$^+$ T cells were isolated from C57BL/6J WT mice using respective naive T cell isolation kits (Miltenyi Biotec). For suppression assays, FACS-sorted B cell subpopulations were cocultured with purified naive T cells (3 × 10^5 B cells to 6 × 10^5 T cells) in 48-well plates that had been precoated with anti-CD3 (10 μg/ml; clone 145-2C11, eBioscience) for 48 hours. During the last 5 hours, PMA/ionomycin plus brefeldin A and monensin was added to the cultures. Cells were subjected to surface and intracellular FACS staining and analyzed by flow cytometry.

Statistics. Data are presented as mean values ± SEM. Statistical analysis was performed using GraphPad Prism (version 6.0h, Mac OS X). Unless stated otherwise, differences between means were assessed using 2-tailed Student's *t* test. Statistical analysis of Kaplan-Meier survival curves was performed by the log-rank test. A *P* value of less than 0.05 was considered statistically significant.

Author contributions

KHL designed the study. JY and VHHD performed the majority of the experiments, with specific contributions by AW, AS, and GAG. Technical assistance was provided by KW. KB provided valuable resources. ACC provided key reagents and feedback on the manuscript. NF and KHL supervised the study, analyzed data, and wrote the manuscript. Funding acquisition was handled by KHL.

Acknowledgments

Address correspondence to: Kyeong-Hee Lee, Institute of Clinical Chemistry and Inflammation Research, Hannover Medical School, Carl-Neuberg-Strasse 1, D-30625 Hannover, Germany. Phone: 49.511.532.5285; Email: Lee.Kyeong-Hee@mh-hannover.de.

1. Plitas G, Rudensky AY. Regulatory T cells: differentiation and function. *Cancer Immunol Res*. 2016;4(9):721–725.
2. Wolf SD, Dittel BN, Hardardottir F, Janeway CA. Experimental autoimmune encephalomyelitis induction in genetically B cell-deficient mice. *J Exp Med*. 1996;184(6):2271–2278.
3. Mauri C, Gray D, Mushtaq N, Londei M. Prevention of arthritis by interleukin 10-producing B cells. *J Exp Med*. 2003;197(4):489–501.
4. Evans JG, et al. Novel suppressive function of transitional 2 B cells in experimental arthritis. *J Immunol*. 2007;178(12):7868–7878.
5. Fillatreau S, Sweenie CH, McGeachy MJ, Gray D, Anderton SM. B cells regulate autoimmunity by provision of IL-10. *Nat Immunol*. 2002;3(10):944–950.
6. Matsushita T, Yanaba K, Bouaziz JD, Fujimoto M, Tedder TF. Regulatory B cells inhibit EAE initiation in mice while other B cells promote disease progression. *J Clin Invest*. 2008;118(10):3420–3430.
7. Mizoguchi A, Mizoguchi E, Takedatsu H, Blumberg RS, Bhan AK. Chronic intestinal inflammatory condition generates IL-10-producing regulatory B cell subset characterized by CD1d upregulation. *Immunity*. 2002;16(2):219–230.
8. Yang M, et al. IL-10-producing regulatory B10 cells ameliorate collagen-induced arthritis via suppressing Th17 cell generation. *Am J Pathol*. 2012;180(6):2375–2385.
9. Lee KM, et al. Anti-CD45RB/anti-TIM-1-induced tolerance requires regulatory B cells. *Am J Transplant*. 2012;12(8):2072–2078.
10. Horikawa M, et al. Regulatory B cell (B10 Cell) expansion during Listeria infection governs innate and cellular immune responses in mice. *J Immunol*. 2013;190(3):1158–1168.
11. Inoue S, Leitner WW, Golding B, Scott D. Inhibitory effects of B cells on antitumor immunity. *Cancer Res*. 2006;66(15):7741–7747.
12. Tedder TF. B10 cells: a functionally defined regulatory B cell subset. *J Immunol*. 2015;194(4):1395–1401.
13. Mauri C, Menon M. The expanding family of regulatory B cells. *Int Immunol*. 2015;27(10):479–486.
14. Vire B, David A, Wiestner A. TOSO, the Fcmicro receptor, is highly expressed on chronic lymphocytic leukemia B cells, internalizes upon IgM

binding, shuttles to the lysosome, and is downregulated in response to TLR activation. *J Immunol*. 2011;187(8):4040–4050.
15. Pallasch CP, et al. Overexpression of TOSO in CLL is triggered by B-cell receptor signaling and associated with progressive disease. *Blood*. 2008;112(10):4213–4219.
16. Proto-Siqueira R, et al. SAGE analysis demonstrates increased expression of TOSO contributing to Fas-mediated resistance in CLL. *Blood*. 2008;112(2):394–397.
17. Hitoshi Y, et al. Toso, a cell surface, specific regulator of Fas-induced apoptosis in T cells. *Immunity*. 1998;8(4):461–471.
18. Nguyen XH, et al. Toso regulates the balance between apoptotic and nonapoptotic death receptor signaling by facilitating RIP1 ubiquitination. *Blood*. 2011;118(3):598–608.
19. Kubagawa H, et al. Identity of the elusive IgM Fc receptor (FcR) in humans. *J Exp Med*. 2009;206(12):2779–2793.
20. Shima H, et al. Identification of TOSO/FAIM3 as an Fc receptor for IgM. *Int Immunol*. 2010;22(3):149–156.
21. Nguyen TT, et al. The IgM receptor FcμR limits tonic BCR signaling by regulating expression of the IgM BCR. *Nat Immunol*. 2017;18(3):321–333.
22. Ouchida R, et al. FcμR interacts and cooperates with the B cell receptor To promote B cell survival. *J Immunol*. 2015;194(7):3096–3101.
23. Choi SC, et al. Mouse IgM Fc receptor, FCMR, promotes B cell development and modulates antigen-driven immune responses. *J Immunol*. 2013;190(3):987–996.
24. Honjo K, et al. Altered Ig levels and antibody responses in mice deficient for the Fc receptor for IgM (FcμR). *Proc Natl Acad Sci U S A*. 2012;109(39):15882–15887.
25. Ouchida R, et al. Critical role of the IgM Fc receptor in IgM homeostasis, B-cell survival, and humoral immune responses. *Proc Natl Acad Sci U S A*. 2012;109(40):E2699–E2706.
26. Wang H, Coligan JE, Morse HC. Emerging functions of natural IgM and its Fc receptor FCMR in immune homeostasis. *Front Immunol*. 2016;7:99.
27. Lang KS, et al. Involvement of Toso in activation of monocytes, macrophages, and granulocytes. *Proc Natl Acad Sci U S A*. 2013;110(7):2593–2598.
28. Lang PA, et al. Toso regulates differentiation and activation of inflammatory dendritic cells during

persistence-prone virus infection. *Cell Death Differ*. 2015;22(1):164–173.
29. Brenner D, et al. Toso controls encephalitogenic immune responses by dendritic cells and regulatory T cells. *Proc Natl Acad Sci U S A*. 2014;111(3):1060–1065.
30. Thomas PG, Keating R, Hulse-Post DJ, Doherty PC. Cell-mediated protection in influenza infection. *Emerg Infect Dis*. 2006;12(1):48–54.
31. La Gruta NL, Turner SJ. T cell mediated immunity to influenza: mechanisms of viral control. *Trends Immunol*. 2014;35(8):396–402.
32. Sharpe AH, Wherry EJ, Ahmed R, Freeman GJ. The function of programmed cell death 1 and its ligands in regulating autoimmunity and infection. *Nat Immunol*. 2007;8(3):239–245.
33. Grassl GA, Valdez Y, Bergstrom KS, Vallance BA, Finlay BB. Chronic enteric salmonella infection in mice leads to severe and persistent intestinal fibrosis. *Gastroenterology*. 2008;134(3):768–780.
34. Yanaba K, et al. A regulatory B cell subset with a unique CD1d^{hiCD5+} phenotype controls T cell-dependent inflammatory responses. *Immunity*. 2008;28(5):639–650.
35. Mauri C, Bosma A. Immune regulatory function of B cells. *Annu Rev Immunol*. 2012;30:221–241.
36. Candando KM, Lykken JM, Tedder TF. B10 cell regulation of health and disease. *Immunol Rev*. 2014;259(1):259–272.
37. Kaku H, Cheng KF, Al-Abed Y, Rothstein TL. A novel mechanism of B cell-mediated immune suppression through CD73 expression and adenosine production. *J Immunol*. 2014;193(12):5904–5913.
38. Casola S. Control of peripheral B-cell development. *Curr Opin Immunol*. 2007;19(2):143–149.
39. Hardy RR, Hayakawa K. Selection of natural autoreactive B cells. *Clin Exp Rheumatol*. 2015;33(4 suppl 92):S80–S86.
40. Pao LI, et al. B cell-specific deletion of protein-tyrosine phosphatase Shp1 promotes B-1a cell development and causes systemic autoimmunity. *Immunity*. 2007;27(1):35–48.
41. Srinivasan L, et al. PI3 kinase signals BCR-dependent mature B cell survival. *Cell*. 2009;139(3):573–586.
42. Sun K, Torres L, Metzger DW. A detrimental effect of interleukin-10 on protective pulmonary humoral immunity during primary influenza A virus infection. *J Virol*. 2010;84(10):5007–5014.

43. McKinstry KK, et al. IL-10 deficiency unleashes an influenza-specific Th17 response and enhances survival against high-dose challenge. *J Immunol*. 2009;182(12):7353–7363.

44. Madan R, et al. Nonredundant roles for B cell–derived IL-10 in immune counter-regulation. *J Immunol*. 2009;183(4):2312–2320.

45. O'Garra A, Chang R, Go N, Hastings R, Haughton G, Howard M. Ly-1 B (B-1) cells are the main source of B cell–derived interleukin 10. *Eur J Immunol*. 1992;22(3):711–717.

46. Watanabe R, et al. Regulatory B cells (B10 cells) have a suppressive role in murine lupus: CD19 and B10 cell deficiency exacerbates systemic autoimmunity. *J Immunol*. 2010;184(9):4801–4809.

47. Blair PA, et al. CD19(+)CD24(hi)CD38(hi) B cells exhibit regulatory capacity in healthy individuals but are functionally impaired in systemic lupus erythematosus patients. *Immunity*. 2010;32(1):129–140.

48. Ray A, Basu S, Williams CB, Salzman NH, Dittel BN. A novel IL-10-independent regulatory role for B cells in suppressing autoimmunity by maintenance of regulatory T cells via GITR ligand. *J Immunol*. 2012;188(7):3188–3198.

49. Lundy SK, Fox DA. Reduced Fas ligand-expressing splenic CD5+ B lymphocytes in severe collagen-induced arthritis. *Arthritis Res Ther*. 2009;11(4):R128.

50. Natarajan P, et al. Regulatory B cells from hilar lymph nodes of tolerant mice in a murine model of allergic airway disease are CD5+, express TGF-β, and co-localize with CD4+Foxp3+ T cells. *Mucosal Immunol*. 2012;5(6):691–701.

51. Shen P, et al. IL-35-producing B cells are critical regulators of immunity during autoimmune and infectious diseases. *Nature*. 2014;507(7492):366–370.

52. Bendelac A, Bonneville M, Kearney JF. Autoreactivity by design: innate B and T lymphocytes. *Nat Rev Immunol*. 2001;1(3):177–186.

53. Lee CC, Kung JT. Marginal zone B cell is a major source of Il-10 in Listeria monocytogenes susceptibility. *J Immunol*. 2012;189(7):3319–3327.

54. Bankoti R, Gupta K, Levchenko A, Stäger S. Marginal zone B cells regulate antigen-specific T cell responses during infection. *J Immunol*. 2012;188(8):3961–3971.

55. Sindhava V, Woodman ME, Stevenson B, Bondada S. Interleukin-10 mediated autoregulation of murine B-1 B-cells and its role in Borrelia hermsii infection. *PLoS One*. 2010;5(7):e11445.

56. Zhang X, Deriaud E, Jiao X, Braun D, Leclerc C, Lo-Man R. Type I interferons protect neonates from acute inflammation through interleukin 10-producing B cells. *J Exp Med*. 2007;204(5):1107–1118.

57. Shimomura Y, et al. Regulatory role of B-1 B cells in chronic colitis. *Int Immunol*. 2008;20(6):729–737.

58. Miles K, et al. A tolerogenic role for Toll-like receptor 9 is revealed by B-cell interaction with DNA complexes expressed on apoptotic cells. *Proc Natl Acad Sci U S A*. 2012;109(3):887–892.

59. Gray M, Miles K, Salter D, Gray D, Savill J. Apoptotic cells protect mice from autoimmune inflammation by the induction of regulatory B cells. *Proc Natl Acad Sci U S A*. 2007;104(35):14080–14085.

60. Enghard P, et al. Class switching and consecutive loss of dsDNA-reactive B1a B cells from the peritoneal cavity during murine lupus development. *Eur J Immunol*. 2010;40(6):1809–1818.

61. Takahashi T, Strober S. Natural killer T cells and innate immune B cells from lupus-prone NZB/W mice interact to generate IgM and IgG autoantibodies. *Eur J Immunol*. 2008;38(1):156–165.

62. Haas KM, et al. Protective and pathogenic roles for B cells during systemic autoimmunity in NZB/W F1 mice. *J Immunol*. 2010;184(9):4789–4800.

63. Valdez Y, et al. Nramp1 drives an accelerated inflammatory response during Salmonella-induced colitis in mice. *Cell Microbiol*. 2009;11(2):351–362.